

Study of the $B_c^+ \rightarrow J/\psi D_s^+$ and $B_c^+ \rightarrow J/\psi D_s^{*+}$ decays with the ATLAS detector

ATLAS Collaboration*

CERN, 1211 Geneva 23, Switzerland

Received: 27 July 2015 / Accepted: 19 October 2015 / Published online: 5 January 2016

© CERN for the benefit of the ATLAS collaboration 2015. This article is published with open access at Springerlink.com

Abstract The decays $B_c^+ \rightarrow J/\psi D_s^+$ and $B_c^+ \rightarrow J/\psi D_s^{*+}$ are studied with the ATLAS detector at the LHC using a dataset corresponding to integrated luminosities of 4.9 and 20.6 fb⁻¹ of pp collisions collected at centre-of-mass energies $\sqrt{s} = 7$ TeV and 8 TeV, respectively. Signal candidates are identified through $J/\psi \rightarrow \mu^+\mu^-$ and $D_s^{(*)+} \rightarrow \phi\pi^+(\gamma/\pi^0)$ decays. With a two-dimensional likelihood fit involving the B_c^+ reconstructed invariant mass and an angle between the μ^+ and D_s^+ candidate momenta in the muon pair rest frame, the yields of $B_c^+ \rightarrow J/\psi D_s^+$ and $B_c^+ \rightarrow J/\psi D_s^{*+}$, and the transverse polarisation fraction in $B_c^+ \rightarrow J/\psi D_s^{*+}$ decay are measured. The transverse polarisation fraction is determined to be $\Gamma_{\pm\pm}(B_c^+ \rightarrow J/\psi D_s^{*+})/\Gamma(B_c^+ \rightarrow J/\psi D_s^{*+}) = 0.38 \pm 0.23 \pm 0.07$, and the derived ratio of the branching fractions of the two modes is $\mathcal{B}_{B_c^+ \rightarrow J/\psi D_s^{*+}}/\mathcal{B}_{B_c^+ \rightarrow J/\psi D_s^+} = 2.8_{-0.8}^{+1.2} \pm 0.3$, where the first error is statistical and the second is systematic. Finally, a sample of $B_c^+ \rightarrow J/\psi\pi^+$ decays is used to derive the ratios of branching fractions $\mathcal{B}_{B_c^+ \rightarrow J/\psi D_s^+}/\mathcal{B}_{B_c^+ \rightarrow J/\psi\pi^+} = 3.8 \pm 1.1 \pm 0.4 \pm 0.2$ and $\mathcal{B}_{B_c^+ \rightarrow J/\psi D_s^{*+}}/\mathcal{B}_{B_c^+ \rightarrow J/\psi\pi^+} = 10.4 \pm 3.1 \pm 1.5 \pm 0.6$, where the third error corresponds to the uncertainty of the branching fraction of $D_s^+ \rightarrow \phi(K^+K^-)\pi^+$ decay. The available theoretical predictions are generally consistent with the measurement.

1 Introduction

The B_c^+ meson¹ is the only known weakly decaying particle consisting of two heavy quarks. The ground $\bar{b}c$ state was first observed by CDF [1] via its semileptonic decay $B_c^+ \rightarrow J/\psi\ell^+\nu_\ell$. An excited $\bar{b}c$ state has been observed recently by ATLAS [2] using the B_c^+ decay mode $B_c^+ \rightarrow J/\psi\pi^+$. The presence of two heavy quarks, each of which can decay weakly, affects theoretical calculations of the decay proper-

ties of the B_c^+ meson. In the case of $\bar{b} \rightarrow \bar{c}c\bar{s}$ processes, decays to charmonium and a D_s^+ or a D_s^{*+} meson are predicted to occur via colour-suppressed and colour-favoured spectator diagrams as well as via the weak annihilation diagram (see Fig. 1). The latter, in contrast to decays of other B mesons, is not Cabibbo-suppressed and can contribute significantly to the decay amplitudes. The decay properties are addressed in various theoretical calculations [3–9] and can also be compared to the analogous properties in the lighter B meson systems such as $B_d^0 \rightarrow D^{*-}D_s^{(*)+}$ or $B^+ \rightarrow \bar{D}^{*0}D_s^{(*)+}$. The decays $B_c^+ \rightarrow J/\psi D_s^+$ and $B_c^+ \rightarrow J/\psi D_s^{*+}$, which have been observed recently by the LHCb experiment [10], provide a means to test these theoretical predictions.

This paper presents a measurement of the branching fractions of $B_c^+ \rightarrow J/\psi D_s^+$ and $B_c^+ \rightarrow J/\psi D_s^{*+}$ decays, normalised to that of $B_c^+ \rightarrow J/\psi\pi^+$ decay, and polarisation in $B_c^+ \rightarrow J/\psi D_s^{*+}$ decay performed with the ATLAS detector [11]. The D_s^+ meson is reconstructed via the $D_s^+ \rightarrow \phi\pi^+$ decay with the ϕ meson decaying into a pair of charged kaons. The D_s^{*+} meson decays into a D_s^+ meson and a soft photon or π^0 . Detecting such soft neutral particles is very challenging, thus no attempt to reconstruct them is made in the analysis. The J/ψ meson is reconstructed via its decay into a muon pair.

The measurement presented in this paper allows an independent verification of the results of Ref. [10] with comparable statistical and systematic uncertainties. The following ratios are measured: $\mathcal{R}_{D_s^+/\pi^+} = \mathcal{B}_{B_c^+ \rightarrow J/\psi D_s^+}/\mathcal{B}_{B_c^+ \rightarrow J/\psi\pi^+}$, $\mathcal{R}_{D_s^{*+}/\pi^+} = \mathcal{B}_{B_c^+ \rightarrow J/\psi D_s^{*+}}/\mathcal{B}_{B_c^+ \rightarrow J/\psi\pi^+}$, and $\mathcal{R}_{D_s^{*+}/D_s^+} = \mathcal{B}_{B_c^+ \rightarrow J/\psi D_s^{*+}}/\mathcal{B}_{B_c^+ \rightarrow J/\psi D_s^+}$, where $\mathcal{B}_{B_c^+ \rightarrow X}$ denotes the branching fraction of the $B_c^+ \rightarrow X$ decay. The decay $B_c^+ \rightarrow J/\psi D_s^{*+}$ is a transition of a pseudoscalar meson into a pair of vector states and is thus described by the three helicity amplitudes, A_{++} , A_{--} , and A_{00} , where the subscripts correspond to the helicities of J/ψ and D_s^{*+} mesons. The contribution of the A_{++} and A_{--} amplitudes, referred to as the $A_{\pm\pm}$ component, corresponds to the J/ψ and D_s^{*+} transverse polarisation. The fraction of transverse polarisation,

¹ Charge conjugate states are implied throughout the paper unless otherwise stated.

* e-mail: atlas.publications@cern.ch

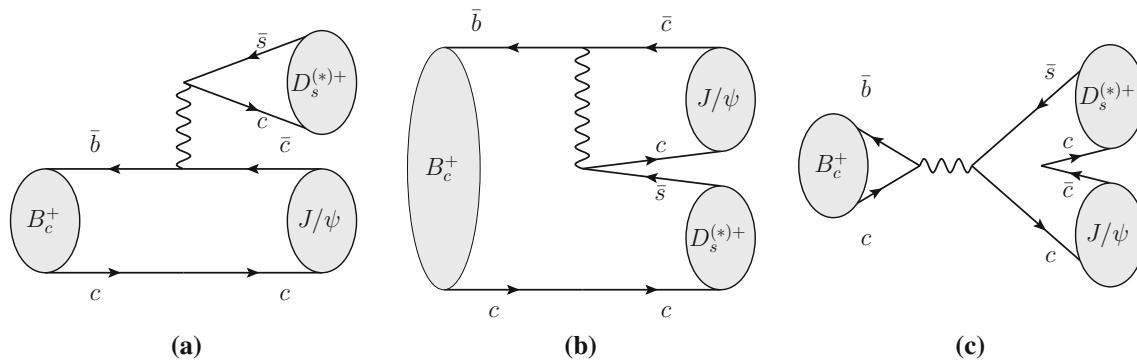


Fig. 1 Feynman diagrams for $B_c^+ \rightarrow J/\psi D_s^{(*)+}$ decays: **a** colour-favoured spectator, **b** colour-suppressed spectator, and **c** annihilation topology

$\Gamma_{\pm\pm}/\Gamma = \Gamma_{\pm\pm}(B_c^+ \rightarrow J/\psi D_s^{(*)+})/\Gamma(B_c^+ \rightarrow J/\psi D_s^{(*)+})$, is also measured. From a naive prediction by spin counting, one would expect this fraction to be $2/3$, while calculations [8,9] predict values of $0.41\text{--}0.48$.

This analysis is based on a combined sample of pp collision data collected by the ATLAS experiment at the LHC at centre-of-mass energies $\sqrt{s} = 7\text{ TeV}$ and 8 TeV corresponding to integrated luminosities of 4.9 and 20.6 fb^{-1} , respectively.

2 The ATLAS detector, trigger selection and Monte Carlo samples

ATLAS is a general-purpose detector consisting of several subsystems including the inner detector (ID), calorimeters and the muon spectrometer (MS). Muon reconstruction makes use of both the ID and the MS. The ID comprises three types of detectors: a silicon pixel detector, a silicon microstrip semiconductor tracker (SCT) and a transition radiation tracker. The ID provides a pseudorapidity² coverage up to $|\eta| = 2.5$. Muons pass through the calorimeters and reach the MS if their transverse momentum, p_T , is above approximately 3 GeV .³ Muon candidates are formed either from a stand-alone MS track matched to an ID track or, in case the MS stand-alone track is not reconstructed, from an ID track extrapolated to the MS and matched to track segments in the MS. Candidates of the latter type are referred to as segment-tagged muons while the former are called combined muons. Muon track parameters are taken from the ID measurement alone in this analysis, since the precision of the measured

track parameters for muons in the p_T range of interest is dominated by the ID track reconstruction.

The ATLAS trigger system consists of a hardware-based Level-1 trigger and a two-stage high level trigger (HLT). At Level-1, the muon trigger uses dedicated MS chambers to search for patterns of hits satisfying different p_T thresholds. The region-of-interest around these hit patterns then serves as a seed for the HLT muon reconstruction, in which dedicated algorithms are used to incorporate information from both the MS and the ID, achieving a position and momentum resolution close to that provided by the offline muon reconstruction. Muons are efficiently triggered in the pseudorapidity range $|\eta| < 2.4$.

Triggers based on single-muon, dimuon, and three-muon signatures are used to select $J/\psi \rightarrow \mu^+\mu^-$ decays for the analysis. The third muon can be produced in the B_c^+ signal events in semileptonic decays of the two other heavy-flavour hadrons. The majority of events are collected by dimuon triggers requiring a vertex of two oppositely charged muons with an invariant mass between 2.5 and 4.3 GeV . During the data taking, the p_T threshold for muons in these triggers was either 4 or 6 GeV . Single-muon triggers additionally increase the acceptance for asymmetric J/ψ decays where one muon has $p_T < 4\text{ GeV}$. Finally, three-muon triggers had a p_T threshold of 4 GeV , thus enhancing the acceptance during the periods of high luminosity when the p_T threshold for at least one muon in the dimuon triggers was 6 GeV .

Monte Carlo (MC) simulation is used for the event selection criteria optimisation and the calculation of the acceptance for the considered B_c^+ decay modes. The MC samples of the B_c^+ decays were generated with PYTHIA 6.4 [12] along with a dedicated extension for the B_c^+ production based on calculations from Refs. [13–16]. The decays of B_c^+ are then simulated with EVTGEN [17]. The generated events were passed through a full simulation of the detector using the ATLAS simulation framework [18] based on GEANT 4 [19,20] and processed with the same reconstruction algorithms as were used for the data.

² ATLAS uses a right-handed coordinate system with its origin at the nominal interaction point (IP) in the centre of the detector and the z -axis along the beam pipe. The x -axis points from the IP to the centre of the LHC ring, and the y -axis points upward. Cylindrical coordinates (r, ϕ) are used in the transverse plane, ϕ being the azimuthal angle around the beam pipe. The pseudorapidity is defined in terms of the polar angle θ as $\eta = -\ln \tan(\theta/2)$.

³ Using a system of units with $c = 1$ is implied throughout the paper.

3 Reconstruction and event selection

The J/ψ candidates are reconstructed from pairs of oppositely charged muons. At least one of the two muons is required to be a combined muon. Each pair is fitted to a common vertex [21]. The quality of the vertex fit must satisfy $\chi^2/\text{ndf} < 15$, where the ndf stands for the number of degrees of freedom. The candidates in the invariant mass window $2800 \text{ MeV} < m(\mu^+\mu^-) < 3400 \text{ MeV}$ are retained.

For the $D_s^+ \rightarrow \phi(K^+K^-)\pi^+$ reconstruction, tracks of particles with opposite charges are assigned kaon mass hypotheses and combined in pairs to form ϕ candidates. An additional track is assigned a pion mass and combined with the ϕ candidate to form a D_s^+ candidate. To ensure good momentum resolution, all three tracks are required to have at least two hits in the silicon pixel detector and at least six hits in the SCT. Only three-track combinations successfully fitted to a common vertex with $\chi^2/\text{ndf} < 8$ are kept. The ϕ candidate invariant mass, $m(K^+K^-)$, and the D_s^+ candidate invariant mass, $m(K^+K^-\pi^+)$, are calculated using the track momenta refitted to the common vertex. Only candidates with $m(K^+K^-)$ within $\pm 7 \text{ MeV}$ around the ϕ mass, $m_\phi = 1019.461 \text{ MeV}$ [22], and with $1930 \text{ MeV} < m(K^+K^-\pi^+) < 2010 \text{ MeV}$ are retained.

The $B_c^+ \rightarrow J/\psi D_s^+$ candidates are built by combining the five tracks of the J/ψ and D_s^+ candidates. The J/ψ meson decays instantly at the same point as the B_c^+ does (secondary vertex) while the D_s^+ lives long enough to form a displaced tertiary vertex. Therefore the five-track combinations are refitted assuming this cascade topology [21]. The invariant mass of the muon pair is constrained to the J/ψ mass, $m_{J/\psi} = 3096.916 \text{ MeV}$ [22]. The three D_s^+ daughter tracks are constrained to a tertiary vertex and their invariant mass is fixed to the mass of D_s^+ , $m_{D_s^+} = 1968.30 \text{ MeV}$ [22]. The combined momentum of the refitted D_s^+ decay tracks is constrained to point to the dimuon vertex. The quality of the cascade fit must satisfy $\chi^2/\text{ndf} < 3$.

The B_c^+ meson is reconstructed within the kinematic range $p_T(B_c^+) > 15 \text{ GeV}$ and $|\eta(B_c^+)| < 2.0$, where the detector acceptance is high and depends weakly on $p_T(B_c^+)$ and $\eta(B_c^+)$.

The refitted tracks of the D_s^+ daughter hadrons are required to have $|\eta| < 2.5$ and $p_T > 1 \text{ GeV}$, while the muons must have $|\eta| < 2.3$ and $p_T > 3 \text{ GeV}$. To further discriminate the sample of D_s^+ candidates from a large combinatorial background, the following requirements are applied:

- $\cos \theta^*(\pi) < 0.8$, where $\theta^*(\pi)$ is the angle between the pion momentum in the $K^+K^-\pi^+$ rest frame and the $K^+K^-\pi^+$ combined momentum in the laboratory frame;
- $|\cos^3 \theta'(K)| > 0.15$, where $\theta'(K)$ is the angle between one of the kaons and the pion in the K^+K^- rest frame.

The decay of the pseudoscalar D_s^+ meson to the ϕ (vector) plus π (pseudoscalar) final state results in an alignment of the spin of the ϕ meson perpendicularly to the direction of motion of the ϕ relative to D_s^+ . Consequently, the distribution of $\cos \theta'(K)$ follows a $\cos^2 \theta'(K)$ shape, implying a uniform distribution for $\cos^3 \theta'(K)$. In contrast, the $\cos \theta'(K)$ distribution of the combinatorial background is uniform and its $\cos^3 \theta'(K)$ distribution peaks at zero. The cut suppresses the background significantly while reducing the signal by 15 %.

The B_c^+ candidate is required to point back to a primary vertex such that $d_0^{\text{PV}}(B_c^+) < 0.1 \text{ mm}$ and $z_0^{\text{PV}}(B_c^+) \sin \theta(B_c^+) < 0.5 \text{ mm}$, where d_0^{PV} and z_0^{PV} are respectively the transverse and longitudinal impact parameters with respect to the primary vertex. All primary vertices in the event are considered. If there is more than one primary vertex satisfying these requirements ($\sim 0.5\%$ events both in data and MC simulation), the one with the largest sum of squared transverse momenta of the tracks originating from it is chosen.

The transverse decay length⁴ of the B_c^+ candidate is required to satisfy $L_{xy}(B_c^+) > 0.1 \text{ mm}$. The transverse decay length of the D_s^+ measured from the B_c^+ vertex must be $L_{xy}(D_s^+) > 0.15 \text{ mm}$. In order to remove fake candidates, both $L_{xy}(B_c^+)$ and $L_{xy}(D_s^+)$ are required not to exceed 10 mm.

Taking into account the characteristic hard fragmentation of b -quarks, a requirement $p_T(B_c^+)/\sum p_T(\text{trk}) > 0.1$ is applied, where the sum in the denominator is taken over all tracks originating from the primary vertex (tracks of the B_c^+ candidate are included in the sum if they are associated with the primary vertex). The requirement reduces a sizeable fraction of combinatorial background while having almost no effect on the signal.

The following angular selection requirements are introduced to further suppress the combinatorial background:

- $\cos \theta^*(D_s^+) > -0.8$, where $\theta^*(D_s^+)$ is the angle between the D_s^+ candidate momentum in the rest frame of the B_c^+ candidate, and the B_c^+ candidate line of flight in the laboratory frame. The distribution of $\cos \theta^*(D_s^+)$ is uniform for the decays of pseudoscalar B_c^+ meson before any kinematic selection while it tends to increase for negative values of $\cos \theta^*(D_s^+)$ for the background.
- $\cos \theta'(\pi) > -0.8$, where $\theta'(\pi)$ is the angle between the J/ψ candidate momentum and the pion momentum in the $K^+K^-\pi^+$ rest frame. Its distribution is nearly uniform for the signal processes but peaks towards -1 for the background.

⁴ The transverse decay length of a particle is defined as the transverse distance between the production (primary) vertex and the particle decay (secondary) vertex projected along its transverse momentum.

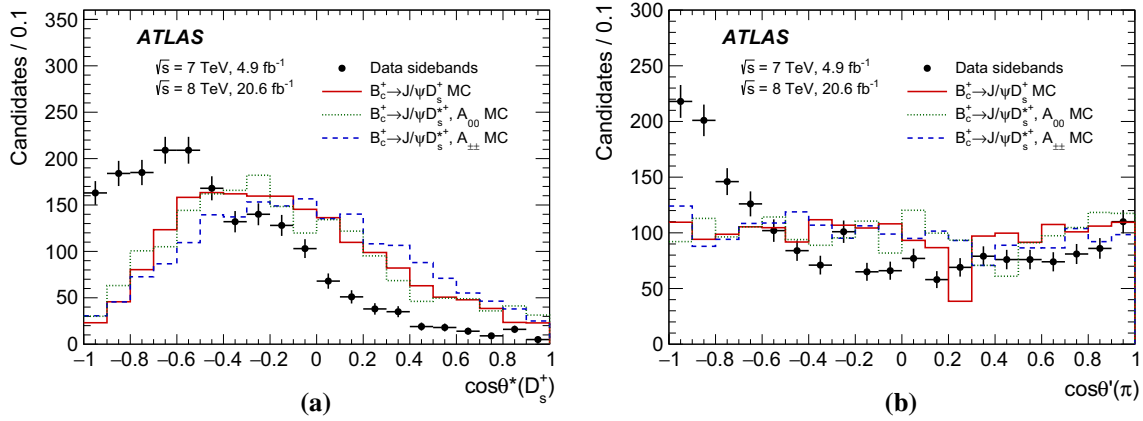


Fig. 2 Distributions of **a** $\cos \theta^*(D_s^+)$ and **b** $\cos \theta'(\pi)$, where $\theta^*(D_s^+)$ and $\theta'(\pi)$ are two angular variables defined in Sect. 3. The distributions are shown for data sidebands (black dots) and MC simulation of $B_c^+ \rightarrow J/\psi D_s^+$ signal (red solid line) and A_{00} (green dotted line) and

$A_{\pm\pm}$ (blue dashed line) components of $B_c^+ \rightarrow J/\psi D_s^{*+}$ signal. The distributions are obtained after applying all selection criteria except the ones on the plotted variable. The MC distributions are normalised to data

Distributions of these two variables after applying all other selection requirements described in this section are shown in Fig. 2. They are shown for the simulated signal samples, as well as for sidebands of the mass spectrum in data, defined as the regions $5640 \text{ MeV} < m(J/\psi D_s^+) < 5900 \text{ MeV}$ (left sideband) and $6360 \text{ MeV} < m(J/\psi D_s^+) < 6760 \text{ MeV}$ (right sideband). A dip in the $\cos \theta'(\pi)$ distribution for the $B_c^+ \rightarrow J/\psi D_s^+$ signal is caused by rejection of $B_s^0 \rightarrow J/\psi \phi$ candidates discussed below.

Various possible contributions of partially reconstructed $B \rightarrow J/\psi X$ decays were studied. The only significant one was found from the $B_s^0 \rightarrow J/\psi \phi$ decay process. This contribution arises when the combination of the tracks from a true $B_s^0 \rightarrow J/\psi(\mu^+\mu^-)\phi(K^+K^-)$ decay with a fifth random track results in a fake $B_c^+ \rightarrow J/\psi(\mu^+\mu^-)D_s^+(K^+K^-\pi^+)$ candidate. For each reconstructed B_c^+ candidate, an additional vertex fit is performed. The two muon tracks and the two kaon tracks are fitted to a common vertex, where the kaon tracks are assumed to be from $\phi \rightarrow K^+K^-$ and the muon pair is constrained to have the nominal J/ψ mass. The mass of the B_s^0 candidate, $m(\mu^+\mu^-K^+K^-)$, is then calculated from the refitted track parameters. Candidates with $5340 \text{ MeV} < m(\mu^+\mu^-K^+K^-) < 5400 \text{ MeV}$ are rejected. This requirement suppresses the bulk of the B_s^0 events while rejecting only $\sim 4\%$ of the signal.

After applying the selection requirements described above, 1547 $J/\psi D_s^+$ candidates are selected in the mass range 5640–6760 MeV.

4 $B_c^+ \rightarrow J/\psi D_s^{(*)+}$ candidate fit

The mass distribution of the selected $B_c^+ \rightarrow J/\psi D_s^{(*)+}$ candidates is shown in Fig. 3. The peak near the B_c^+ mass, $m_{B_c^+} = 6275.6 \text{ MeV}$ [22], is attributed to the signal of

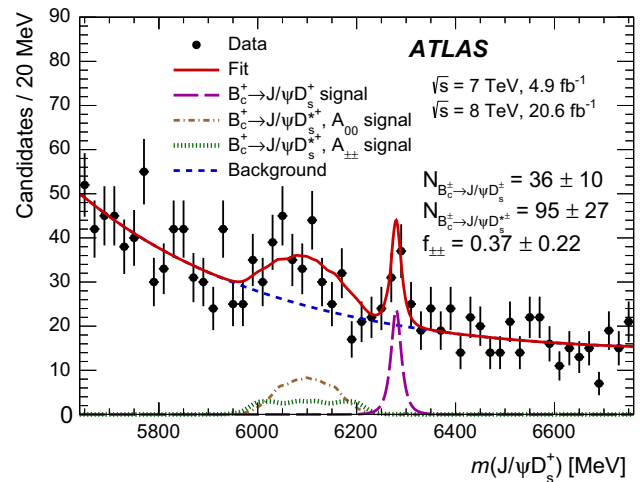


Fig. 3 The mass distribution for the selected $J/\psi D_s^+$ candidates. The red solid line represents the projection of the fit to the model described in the text. The contribution of the $B_c^+ \rightarrow J/\psi D_s^+$ decay is shown with the magenta long-dashed line; the brown dash-dot and green dotted lines show the $B_c^+ \rightarrow J/\psi D_s^{*+} A_{00}$ and $A_{\pm\pm}$ component contributions, respectively; the blue dashed line shows the background model. The uncertainties of the listed fit result values are statistical only

$B_c^+ \rightarrow J/\psi D_s^+$ decay while a wider structure between 5900 and 6200 MeV corresponds to $B_c^+ \rightarrow J/\psi D_s^{*+}$ with subsequent $D_s^{*+} \rightarrow D_s^+\gamma$ or $D_s^{*+} \rightarrow D_s^+\pi^0$ decays where the neutral particle is not reconstructed.

Mass distributions of the J/ψ and D_s^+ candidates corresponding to the $J/\psi D_s^+$ mass region of the observed $B_c^+ \rightarrow J/\psi D_s^{(*)+}$ signals are shown in Fig. 4. To obtain these plots, the B_c^+ candidates are built without the mass constraints in the cascade fit, with the mass of the candidate calculated as $m(J/\psi D_s^+) = m(\mu^+\mu^-K^+K^-\pi^+) - m(\mu^+\mu^-) + m_{J/\psi} - m(K^+K^-\pi^+) + m_{D_s^+}$, where $m_{J/\psi}$ and $m_{D_s^+}$ are the nominal masses of the respective par-

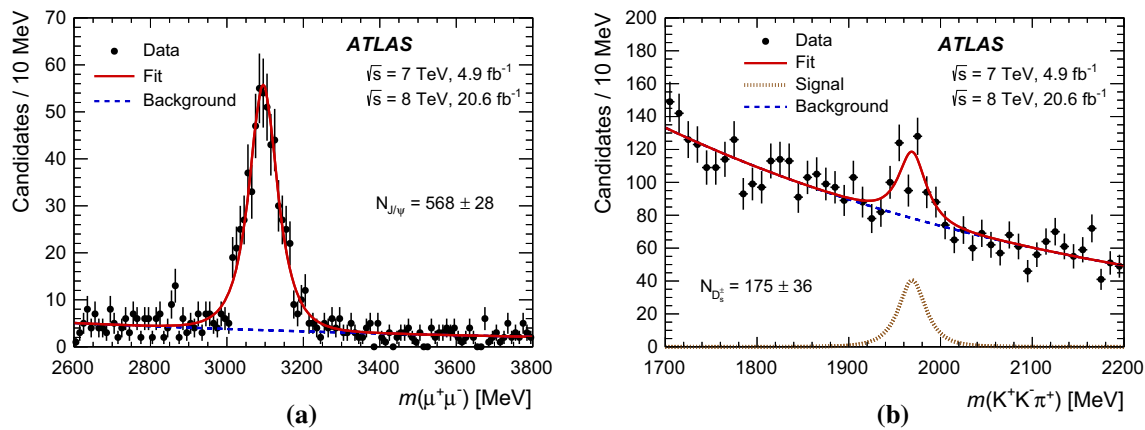


Fig. 4 Mass distribution of the **a** J/ψ and **b** D_s^+ candidates after the full $B_c^+ \rightarrow J/\psi D_s^{*\pm}$ selection (without mass constraints in the cascade fit) in the mass window of the B_c^+ candidate $5900 \text{ MeV} <$

$m(J/\psi D_s^+) < 6400 \text{ MeV}$ while the mass windows for the corresponding intermediate resonances are widened to the plotting ranges. The J/ψ and D_s^+ mass distributions are fitted with a sum of an exponential function describing the background and a modified Gaussian function [23,24] describing the corresponding signal peak. The modified Gaussian function is defined as

$$\text{Gauss}^{\text{mod}} \sim \exp\left(-\frac{x^{1+\frac{1}{1+x/2}}}{2}\right), \quad (1)$$

where $x = |m_0 - m|/\sigma$ with the mean mass m_0 and width σ being free parameters. The fitted masses of J/ψ ($3095.1 \pm 2.4 \text{ MeV}$) and D_s ($1969.0 \pm 4.1 \text{ MeV}$) agree with their nominal masses, the widths are consistent with those in the simulated samples, and the signal yields are found to be $N_{J/\psi} = 568 \pm 28$ and $N_{D_s^\pm} = 175 \pm 36$.

The information about the helicity in $B_c^+ \rightarrow J/\psi D_s^{*\pm}$ decay is encoded both in the mass distribution of the $J/\psi D_s^+$ system and in the distribution of the helicity angle, $\theta'(\mu^+)$, which is defined in the rest frame of the muon pair as the angle between the μ^+ and the D_s^+ candidate momenta. Thus, a two-dimensional extended unbinned maximum-likelihood fit of the $m(J/\psi D_s^+)$ and $|\cos \theta'(\mu^+)|$ distributions is performed. The A_{++} and A_{--} helicity amplitude contributions are described by the same mass and angular shapes because of the parity symmetry of the J/ψ and $D_s^{*\pm}$ decays. This is confirmed by the MC simulation. Thus these components are treated together as the $A_{\pm\pm}$ component, while the shape of the A_{00} component is different and is therefore treated separately. A simultaneous fit to the mass and angular distributions significantly improves the sensitivity to the contributions of the helicity amplitudes in $B_c^+ \rightarrow J/\psi D_s^{*\pm}$ decay with respect to a one-dimensional mass fit.

$m(J/\psi D_s^+) < 6400 \text{ MeV}$. The spectra are fitted with a sum of an exponential and a modified Gaussian function. The uncertainties of the shown J/ψ and D_s^+ yields are statistical only

Four two-dimensional probability density functions (PDFs) are defined to describe the $B_c^+ \rightarrow J/\psi D_s^+$ signal, the $A_{\pm\pm}$ and A_{00} components of the $B_c^+ \rightarrow J/\psi D_s^{*\pm}$ signal, and the background. The signal PDFs are factorised into mass and angular components. The effect of correlations between their mass and angular shapes is found to be small and is accounted for as a systematic uncertainty.

The mass distribution of the $B_c^+ \rightarrow J/\psi D_s^+$ signal is described by a modified Gaussian function. For the $B_c^+ \rightarrow J/\psi D_s^{*\pm}$ signal components, the mass shape templates obtained from the simulation with the kernel estimation technique [25] are used. The branching fractions of $D_s^{*\pm} \rightarrow D_s^+ \pi^0$ and $D_s^{*\pm} \rightarrow D_s^+ \gamma$ decays for the simulation are set to the world average values [22]. The position of the templates along the mass axis is varied in the fit simultaneously with the position of the $B_c^+ \rightarrow J/\psi D_s^+$ signal peak. The background mass shape is described with a two-parameter exponential function, $\exp[a \cdot m(J/\psi D_s^+) + b \cdot m(J/\psi D_s^+)^2]$.

To describe the $|\cos \theta'(\mu^+)|$ shapes, templates from the kernel estimation are used. The templates for the signal angular PDFs are extracted from the simulated samples. Although their shapes are calculable analytically, using the templates allows the fit to account for detector effects. The background angular description is based on the $|\cos \theta'(\mu^+)|$ shape of the candidates in the sidebands of $J/\psi D_s^+$ mass spectra. Two templates are produced from the angular distributions of the candidates in the left and right mass sidebands as defined in Sect. 3. The angular PDF for the background is defined as a conditional PDF of $|\cos \theta'(\mu^+)|$ given the per-candidate $m(J/\psi D_s^+)$. For the candidates in the lower half of the left sideband ($5640\text{--}5770 \text{ MeV}$), the template from the left sideband is used. Similarly, the template from the right sideband is used for the upper half of the right sideband ($6560\text{--}6760 \text{ MeV}$). For the candidates in the middle part of the mass spectrum (5770--

Table 1 Parameters of the $B_c^+ \rightarrow J/\psi D_s^{(*)+}$ signals obtained with the unbinned extended maximum-likelihood fit. The width parameter of the modified Gaussian function is fixed to the MC value. Only statistical uncertainties are shown. No acceptance corrections are applied to the signal yields

| Parameter | Value |
|--|------------------|
| $m_{B_c^+ \rightarrow J/\psi D_s^+}$ (MeV) | 6279.9 ± 3.5 |
| $N_{B_c^+ \rightarrow J/\psi D_s^+}$ | 36 ± 10 |
| $N_{B_c^+ \rightarrow J/\psi D_s^{*+}}$ | 95 ± 27 |
| $f_{\pm\pm}$ | 0.37 ± 0.22 |

6560 MeV), a linear interpolation between the two templates is used.

The fit has seven free parameters: the mass of the B_c^+ meson, $m_{B_c^+ \rightarrow J/\psi D_s^+}$; the relative contribution of the $A_{\pm\pm}$ component to the total $B_c^+ \rightarrow J/\psi D_s^{*+}$ decay rate in the selected sample, $f_{\pm\pm}$; the two parameters of the exponential background; the yields of the two signal modes, $N_{B_c^+ \rightarrow J/\psi D_s^+}$ and $N_{B_c^+ \rightarrow J/\psi D_s^{*+}}$, and the background yield. The width of the modified Gaussian function, $\sigma_{B_c^+ \rightarrow J/\psi D_s^+}$, is fixed to the value obtained from the fit to the simulated signal, $\sigma_{B_c^+ \rightarrow J/\psi D_s^+} = 9.95$ MeV. Leaving this parameter free in the data fit results in the value 7.9 ± 3.0 MeV, consistent with the simulation in the range of statistical uncertainty.

It was checked that the fit procedure provides unbiased values and correct statistical uncertainties for the extracted parameters using pseudo-experiments. The values of the relevant parameters obtained from the fit are given in Table 1. The fitted B_c^+ mass agrees with the world average value [22].

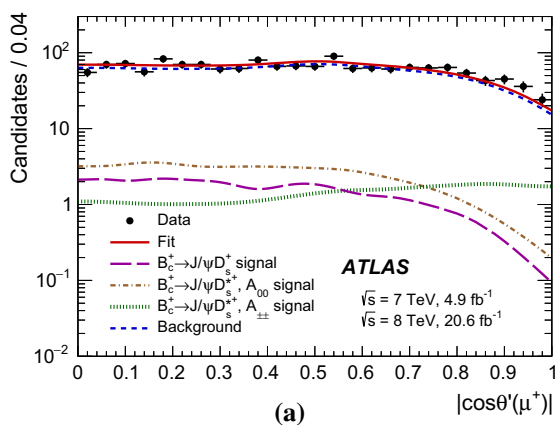


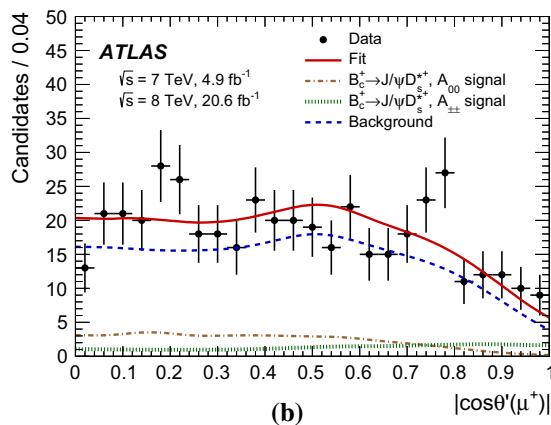
Fig. 5 The projection of the likelihood fit on the variable $|\cos \theta'(\mu^+)|$, where the helicity angle $\theta'(\mu^+)$ is the angle between the μ^+ and D_s^+ candidate momenta in the rest frame of the muon pair from J/ψ decay, for **a** the full selected $J/\psi D_s^+$ candidate dataset and **b** a subset of the candidates in a mass range $5950 \text{ MeV} < m(J/\psi D_s^+) < 6250 \text{ MeV}$ corresponding to the observed signal of $B_c^+ \rightarrow J/\psi D_s^{*+}$ decay. The

mass and angular projections of the fit on the selected $J/\psi D_s^+$ candidate dataset are also shown in Figs. 3 and 5a, respectively. In order to illustrate the effect of the angular part of the fit in separating the helicity amplitudes, the $|\cos \theta'(\mu^+)|$ projection for the subset of candidates with the masses $5950 \text{ MeV} < m(J/\psi D_s^+) < 6250 \text{ MeV}$ corresponding to the region of the observed $B_c^+ \rightarrow J/\psi D_s^{*+}$ signal is shown in Fig. 5b.

The statistical significance for the observed B_c^+ signal estimated from toy MC studies is 4.9 standard deviations.

5 $B_c^+ \rightarrow J/\psi \pi^+$ candidate reconstruction and fit

$B_c^+ \rightarrow J/\psi \pi^+$ candidates are reconstructed by fitting a common vertex of a pion candidate track and the two muons from a J/ψ candidate, selected as described in Sect. 3. For the pion candidate, tracks identified as muons are vetoed in order to suppress the substantial background from $B_c^+ \rightarrow J/\psi \mu^+ \nu_\mu X$ decays. The invariant mass of the two muons in the vertex fit is constrained to the J/ψ nominal mass. The quality of the fit must satisfy $\chi^2/\text{ndf} < 3$. The following selection requirements applied to the $B_c^+ \rightarrow J/\psi \pi^+$ candidates are analogous to those for $B_c^+ \rightarrow J/\psi D_s^+$ candidates described in Sect. 3: the candidates must be within the kinematic range $p_T(B_c^+) > 15 \text{ GeV}$, $|\eta(B_c^+)| < 2.0$; the refitted values of the transverse momenta and pseudorapidities of the muons are required to satisfy $p_T(\mu^\pm) > 3 \text{ GeV}$, $|\eta(\mu^\pm)| < 2.3$; the same requirements on pointing to the primary vertex and the ratio $p_T(B_c^+)/\sum p_T(\text{trk})$ are applied. The refitted pion track kinematics must satisfy $p_T(\pi^+) > 5 \text{ GeV}$ and $|\eta(\pi^+)| < 2.5$. The transverse decay length



red solid line represents the full fit projection. The contribution of the $B_c^+ \rightarrow J/\psi D_s^+$ decay is shown with the *magenta long-dashed line* (it is not drawn in **b** because this contribution vanishes in that mass range); the *brown dash-dot* and *green dotted lines* show the $B_c^+ \rightarrow J/\psi D_s^{*+} A_{00}$ and $A_{\pm\pm}$ component contributions, respectively; the *blue dashed line* shows the background model

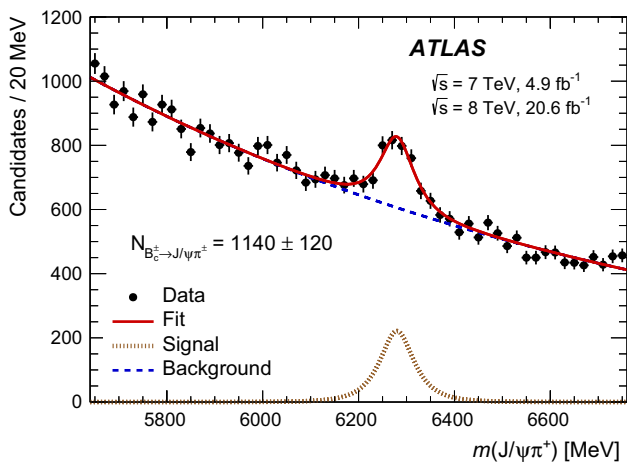


Fig. 6 The mass distribution for the selected $B_c^+ \rightarrow J/\psi\pi^+$ candidates. The red solid line represents the result of the fit to the model described in the text. The brown dotted and blue dashed lines show the signal and background component projections, respectively. The uncertainty of the shown signal yield is statistical only

is required to be $L_{xy}(B_c^+) > 0.2$ mm, and not to exceed 10 mm.

To further suppress combinatorial background, the following selection is applied:

- $\cos\theta^*(\pi) > -0.8$, where $\theta^*(\pi)$ is the angle between the pion momentum in the $\mu^+\mu^-\pi^+$ rest frame and the B_c^+ candidate line of flight in laboratory frame. This angular variable behaviour for the signal and the background is the same as that of $\cos\theta^*(D_s^+)$ used for $J/\psi D_s^+$ candidates selection.
- $|\cos\theta'(\mu^+)| < 0.8$, where $\theta'(\mu^+)$ is the angle between the μ^+ and π^+ momenta in the muon pair rest frame. The signal distribution follows a $\sin^2\theta'(\mu^+)$ shape, while the background is flat.

After applying the above-mentioned requirements, 38542 $J/\psi\pi^+$ candidates are selected in the mass range 5640–6760 MeV. Figure 6 shows the mass distribution of the selected candidates. An extended unbinned maximum-likelihood fit of the mass spectrum is performed to evaluate the $B_c^+ \rightarrow J/\psi\pi^+$ signal yield. The signal contribution is described with the modified Gaussian function while an exponential function is used for the background. The B_c^+ mass, $m_{B_c^+ \rightarrow J/\psi\pi^+}$, the width of the modified Gaussian function, $\sigma_{B_c^+ \rightarrow J/\psi\pi^+}$, the yields of the signal, $N_{B_c^+ \rightarrow J/\psi\pi^+}$, and the background, and the slope of the exponential background are free parameters of the fit. The fit results are summarised in Table 2, and the fit projection is also shown in Fig. 6. The extracted B_c^+ mass value is consistent with the world average [22], and the signal peak width agrees with the simulation (37.4 MeV).

Table 2 Signal parameters of the $J/\psi\pi^+$ mass distribution obtained with the unbinned extended maximum-likelihood fit. Only statistical uncertainties are shown. No acceptance corrections are applied to the signal yields

| Parameter | Value |
|--|------------------|
| $m_{B_c^+ \rightarrow J/\psi\pi^+}$ (MeV) | 6279.9 ± 3.9 |
| $\sigma_{B_c^+ \rightarrow J/\psi\pi^+}$ (MeV) | 33.9 ± 4.2 |
| $N_{B_c^+ \rightarrow J/\psi\pi^+}$ | 1140 ± 120 |

6 Branching fractions and polarisation measurement

The ratios of the branching fractions $\mathcal{R}_{D_s^+/\pi^+}$ and $\mathcal{R}_{D_s^{*+}/\pi^+}$ are calculated as

$$\mathcal{R}_{D_s^{(*)+}/\pi^+} = \frac{\mathcal{B}_{B_c^+ \rightarrow J/\psi D_s^{(*)+}}}{\mathcal{B}_{B_c^+ \rightarrow J/\psi\pi^+}} = \frac{1}{\mathcal{B}_{D_s^+ \rightarrow \phi(K^+K^-)\pi^+}} \times \frac{\mathcal{A}_{B_c^+ \rightarrow J/\psi\pi^+}}{\mathcal{A}_{B_c^+ \rightarrow J/\psi D_s^{(*)+}}} \times \frac{N_{B_c^+ \rightarrow J/\psi D_s^{(*)+}}}{N_{B_c^+ \rightarrow J/\psi\pi^+}}, \quad (2)$$

where $\mathcal{A}_{B_c^+ \rightarrow X}$ and $N_{B_c^+ \rightarrow X}$ are the total acceptance and the yield of the corresponding mode. For $\mathcal{B}_{D_s^+ \rightarrow \phi(K^+K^-)\pi^+}$, the CLEO measurement [26] of the partial $D_s^+ \rightarrow K^+K^-\pi^+$ branching fractions, with a kaon-pair mass within various intervals around the nominal ϕ meson mass, is used. An interpolation between the partial branching fractions, measured for ± 5 and ± 10 MeV intervals, using a relativistic Breit–Wigner shape of the resonance yields the value $(1.85 \pm 0.11)\%$ for the ± 7 MeV interval which is used in the analysis. The effect of admixture of other D_s^+ decay modes with $(K^+K^-\pi^+)$ final state which are not present in the MC simulation is studied separately and accounted for as a systematic uncertainty.

The acceptance for the $B_c^+ \rightarrow J/\psi D_s^{*+}$ decay mode is different for the $A_{\pm\pm}$ and A_{00} components, thus the full acceptance for the mode is

$$\mathcal{A}_{B_c^+ \rightarrow J/\psi D_s^{*+}} = \left(\frac{f_{\pm\pm}}{\mathcal{A}_{B_c^+ \rightarrow J/\psi D_s^{*+}, A_{\pm\pm}}} + \frac{1 - f_{\pm\pm}}{\mathcal{A}_{B_c^+ \rightarrow J/\psi D_s^{*+}, A_{00}}} \right)^{-1}, \quad (3)$$

where the subscripts indicate the helicity state and $f_{\pm\pm}$ is the value extracted from the fit (Table 1). The acceptances are determined from the simulation and shown in Table 3.

The ratio $\mathcal{R}_{D_s^{*+}/D_s^+}$ is calculated as

$$\mathcal{R}_{D_s^{*+}/D_s^+} = \frac{\mathcal{B}_{B_c^+ \rightarrow J/\psi D_s^{*+}}}{\mathcal{B}_{B_c^+ \rightarrow J/\psi D_s^+}} = \frac{N_{B_c^+ \rightarrow J/\psi D_s^{*+}}}{N_{B_c^+ \rightarrow J/\psi D_s^+}} \times \frac{\mathcal{A}_{B_c^+ \rightarrow J/\psi D_s^+}}{\mathcal{A}_{B_c^+ \rightarrow J/\psi D_s^{*+}}}, \quad (4)$$

Table 3 The acceptance $\mathcal{A}_{B_c^+ \rightarrow X}$ for all decay modes studied. Only uncertainties due to MC statistics are shown

| Mode | $\mathcal{A}_{B_c^+ \rightarrow X}$ (%) |
|---|---|
| $B_c^+ \rightarrow J/\psi\pi^+$ | 4.106 ± 0.056 |
| $B_c^+ \rightarrow J/\psi D_s^+$ | 1.849 ± 0.034 |
| $B_c^+ \rightarrow J/\psi D_s^{*+}, A_{00}$ | 1.829 ± 0.053 |
| $B_c^+ \rightarrow J/\psi D_s^{*+}, A_{\pm\pm}$ | 1.712 ± 0.035 |

where the ratio of the yields $N_{B_c^+ \rightarrow J/\psi D_s^{*+}}/N_{B_c^+ \rightarrow J/\psi D_s^+}$ and its uncertainty is extracted from the fit as a parameter in order to account for correlations between the yields.

The fraction of the $A_{\pm\pm}$ component contribution in $B_c^+ \rightarrow J/\psi D_s^{*+}$ decay is calculated from the $f_{\pm\pm}$ value quoted in Table 1 by applying a correction to account for the different acceptances for the two component contributions:

$$\Gamma_{\pm\pm}/\Gamma = f_{\pm\pm} \times \frac{\mathcal{A}_{B_c^+ \rightarrow J/\psi D_s^{*+}}}{\mathcal{A}_{B_c^+ \rightarrow J/\psi D_s^{*+}, A_{\pm\pm}}}. \quad (5)$$

7 Systematic uncertainties

The systematic uncertainties of the measured values are determined by varying the analysis procedure and repeating all calculations. Although some sources can have rather large effects on the individual decay rate measurements, they largely cancel in the ratios of the branching fractions due to correlation between the effects on the different decay modes. The following groups of systematic uncertainties are considered.

The first group of sources of systematic uncertainty relates to possible differences between the data and simulation affecting the acceptances for the decay modes. Thus, an effect of the B_c^+ production model is evaluated by varying the simulated p_T and $|\eta|$ spectra while preserving agreement with the data distributions obtained using the abundant $B_c^+ \rightarrow J/\psi\pi^+$ channel. These variations have very similar effects on the acceptances for the different decay modes, thus giving rather moderate estimates of the uncertainties, not exceeding 3 % in total, on the ratios of branching fractions. The effect of presence of other D_s^+ decay modes with $(K^+K^-\pi^+)$ final state on the calculated acceptances is studied with a separate MC simulation. Its conservative estimate yields 0.4 % which is assigned as $\mathcal{R}_{D_s^+/\pi^+}$ and $\mathcal{R}_{D_s^{*+}/\pi^+}$ uncertainties. An uncertainty on the tracking efficiency is dominated by the uncertainty of the detector material description in the MC simulation. Samples generated with distorted geometries and with increased material are used to estimate the effect on track reconstruction efficiencies. When propagated to the ratios of branching fractions, these estimates give 0.5 % uncertainty for $\mathcal{R}_{D_s^+/\pi^+}$ and $\mathcal{R}_{D_s^{*+}/\pi^+}$ due to

the two extra tracks in $B_c^+ \rightarrow J/\psi D_s^{(*)+}$ modes. Limited knowledge of the B_c^+ and D_s^+ lifetimes leads to an additional systematic uncertainty. The simulated proper decay times are varied within one standard deviation from the world average values [22] resulting in uncertainties of ~ 1 % assigned to $\mathcal{R}_{D_s^+/\pi^+}$ and $\mathcal{R}_{D_s^{*+}/\pi^+}$ due to the B_c^+ lifetime, and 0.3 % due to the D_s^+ lifetime. Removing the requirement on $p_T(B_c^+)/\sum p_T(\text{trk})$ is found to produce no noticeable effect on the measured values.

The next group of uncertainties originates from the signal extraction procedure. These uncertainties are evaluated separately for $J/\psi D_s^+$ and $J/\psi\pi^+$ candidate fits. For the former, the following variations of the fit model are applied and the difference is treated as a systematic uncertainty:

- different background mass shape parametrisations (three-parameter exponential, second- and third-order polynomials), different fitted mass range (reduced by up to 40 MeV from each side independently);
- a double Gaussian or double-sided Crystal Ball function [27–29] for $B_c^+ \rightarrow J/\psi D_s^+$ signal description; variation of the modified Gaussian width within 10 % of the MC simulation value;
- variation of the smoothness of the $B_c^+ \rightarrow J/\psi D_s^{*+}$ signal mass templates, which is controlled by a parameter of the kernel estimation procedure [25];
- similar variation of the smoothness of the $B_c^+ \rightarrow J/\psi D_s^{(*)+}$ signal angular templates;
- variation of the smoothness of the sideband templates used for the background angular PDF construction; different ranges of the sidebands; different sideband interpolation procedure;
- modelling of the correlation between the mass and angular parts of the signal PDFs. This correlation takes place only at the detector level and manifests itself in degradation of the mass resolution for higher values of $|\cos\theta'(\mu^+)|$. A dedicated fit model accounting for this effect is used for the data fit. The impact on the result is found to be negligible compared to the total uncertainty.

The first two items give the dominant contributions to the uncertainties of the ratios of branching fractions while the transverse polarisation fraction measurement is mostly affected by the background angular modelling variations. For the normalisation channel fit model, the similar variations of the background and signal mass shape parametrisation are applied. The deviations produced by the variations of the fits reach values as high as 10–15 % thus making them the dominant sources of systematic uncertainty.

The branching fractions of D_s^{*+} [22] are varied in simulation within their uncertainties to estimate their effect on the measured quantities. Very small uncertainties are obtained

Table 4 Relative systematic uncertainties on the measured ratios of branching fractions $R_{D_s^+/\pi^+}$, $R_{D_s^{*+}/\pi^+}$, $R_{D_s^{*+}/D_s^+}$ and on the transverse polarisation fraction $\Gamma_{\pm\pm}/\Gamma$

| Source | Uncertainty (%) | | | |
|---|-------------------|----------------------|----------------------|--------------------------|
| | $R_{D_s^+/\pi^+}$ | $R_{D_s^{*+}/\pi^+}$ | $R_{D_s^{*+}/D_s^+}$ | $\Gamma_{\pm\pm}/\Gamma$ |
| Simulated $p_T(B_c^+)$ spectrum | 0.4 | 0.9 | 0.5 | 0.4 |
| Simulated $ \eta(B_c^+) $ spectrum | 1.9 | 2.4 | 0.6 | 0.2 |
| Other D_s^+ decay modes contribution | 0.4 | 0.4 | – | – |
| Tracking efficiency | 0.5 | 0.5 | <0.1 | <0.1 |
| B_c^+ lifetime | 1.2 | 1.3 | <0.1 | <0.1 |
| D_s^+ lifetime | 0.3 | 0.3 | <0.1 | <0.1 |
| $B_c^+ \rightarrow J/\psi D_s^{(*)+}$ signal extraction | 4.4 | 10.5 | 10.7 | 17.4 |
| $B_c^+ \rightarrow J/\psi \pi^+$ signal extraction | 8.5 | 8.5 | – | – |
| D_s^{*+} branching fractions | <0.1 | <0.1 | <0.1 | 1.1 |
| MC sample sizes | 2.3 | 2.4 | 2.7 | 2.2 |
| Total | 10.1 | 14.0 | 11.0 | 17.6 |
| $\mathcal{B}_{D_s^+ \rightarrow \phi(K^+K^-)\pi^+}$ | 5.9 | 5.9 | – | – |

for the $\mathcal{R}_{D_s^{*+}/\pi^+}$ and $\mathcal{R}_{D_s^{*+}/D_s^+}$, while for $\Gamma_{\pm\pm}/\Gamma$, the estimate is $\sim 1\%$.

The statistical uncertainties on the acceptance values due to the MC sample sizes are also treated as a separate source of systematic uncertainty and estimated to be 2–3%.

In order to check for a possible bias from using three-muon triggers, vetoing the D_s^+ meson daughter tracks identified as muons is tested and found not to affect the measurement.

Finally, since $\mathcal{B}_{D_s^+ \rightarrow \phi(K^+K^-)\pi^+}$ enters Eq. (2), its uncertainty, evaluated from Ref. [26] as 5.9%, is propagated to the final values of the relative branching fractions.

The systematic uncertainties on the measured quantities are summarised in Table 4.

8 Results

The following ratios of the branching fractions are measured:

$$\begin{aligned} \mathcal{R}_{D_s^+/\pi^+} &= \frac{\mathcal{B}_{B_c^+ \rightarrow J/\psi D_s^+}}{\mathcal{B}_{B_c^+ \rightarrow J/\psi \pi^+}} \\ &= 3.8 \pm 1.1(\text{stat.}) \pm 0.4(\text{syst.}) \pm 0.2(\text{BF}), \end{aligned} \quad (6)$$

$$\begin{aligned} \mathcal{R}_{D_s^{*+}/\pi^+} &= \frac{\mathcal{B}_{B_c^+ \rightarrow J/\psi D_s^{*+}}}{\mathcal{B}_{B_c^+ \rightarrow J/\psi \pi^+}} \\ &= 10.4 \pm 3.1(\text{stat.}) \pm 1.5(\text{syst.}) \pm 0.6(\text{BF}), \end{aligned} \quad (7)$$

$$\begin{aligned} \mathcal{R}_{D_s^{*+}/D_s^+} &= \frac{\mathcal{B}_{B_c^+ \rightarrow J/\psi D_s^{*+}}}{\mathcal{B}_{B_c^+ \rightarrow J/\psi D_s^+}} \\ &= 2.8_{-0.8}^{+1.2}(\text{stat.}) \pm 0.3(\text{syst.}), \end{aligned} \quad (8)$$

where the BF uncertainty corresponds to the knowledge of $\mathcal{B}_{D_s^+ \rightarrow \phi(K^+K^-)\pi^+}$. The relative contribution of the $A_{\pm\pm}$ component in $B_c^+ \rightarrow J/\psi D_s^{*+}$ decay is measured to be

$$\Gamma_{\pm\pm}/\Gamma = 0.38 \pm 0.23(\text{stat.}) \pm 0.07(\text{syst.}) \quad (9)$$

These results are compared with those of the LHCb measurement [10] and to the expectations from various theoretical calculations in Table 5 and Fig. 7. The measurement agrees with the LHCb result. All ratios are well described by the recent perturbative QCD predictions [8]. The expectations from models in Refs. [3, 5, 7] as well as the sum-rules prediction [4] for the ratio $\mathcal{R}_{D_s^{*+}/D_s^+}$ are consistent with the measurement. The QCD relativistic potential model predictions [3] are consistent with the measured $\mathcal{R}_{D_s^+/\pi^+}$ ratio while the expectations from the sum rules [4] and models in Refs. [5–7] are somewhat smaller than the measured value. The predictions in Refs. [3–5, 7] are also generally smaller than the measured ratio $\mathcal{R}_{D_s^{*+}/\pi^+}$; however, the discrepancies do not exceed two standard deviations when taking into account only the experimental uncertainty.

The measured fraction of the $A_{\pm\pm}$ component agrees well with the prediction of the relativistic independent quark model [9] and perturbative QCD [8].

9 Conclusion

A study of $B_c^+ \rightarrow J/\psi D_s^+$ and $B_c^+ \rightarrow J/\psi D_s^{*+}$ decays has been performed. The ratios of the branching fractions $\mathcal{B}_{B_c^+ \rightarrow J/\psi D_s^+}/\mathcal{B}_{B_c^+ \rightarrow J/\psi \pi^+}$, $\mathcal{B}_{B_c^+ \rightarrow J/\psi D_s^{*+}}/\mathcal{B}_{B_c^+ \rightarrow J/\psi \pi^+}$, $\mathcal{B}_{B_c^+ \rightarrow J/\psi D_s^{*+}}/\mathcal{B}_{B_c^+ \rightarrow J/\psi D_s^+}$ and the transverse polarisation fraction of $B_c^+ \rightarrow J/\psi D_s^{*+}$ decay have been measured by the ATLAS experiment at the LHC using pp collision data corresponding to an integrated luminosity of 4.9 fb^{-1} at 7 TeV centre-of-mass energy and 20.6 fb^{-1} at 8 TeV. The polarisation is found to be well described by the available

Table 5 Comparison of the results of this measurement with those of LHCb [10] and theoretical predictions based on a QCD relativistic potential model [3], QCD sum rules [4], relativistic constituent quark model (RCQM) [5], BSW relativistic quark model (with fixed average transverse quark momentum $\omega = 0.40\text{ GeV}$) [6], light-front quark

model (LFQM) [7], perturbative QCD (pQCD) [8], and relativistic independent quark model (RIQM) [9]. The uncertainties of the theoretical predictions are shown if they are explicitly quoted in the corresponding papers. Statistical and systematic uncertainties added in quadrature are shown for the results of ATLAS and LHCb

| $\mathcal{R}_{D_s^+/\pi^+}$ | $\mathcal{R}_{D_s^{*+}/\pi^+}$ | $\mathcal{R}_{D_s^{*+}/D_s^+}$ | $\Gamma_{\pm\pm}/\Gamma$ | Ref. |
|-----------------------------|--------------------------------|--------------------------------|--------------------------|-------------------------|
| 3.8 ± 1.2 | 10.4 ± 3.5 | $2.8^{+1.2}_{-0.9}$ | 0.38 ± 0.24 | ATLAS |
| 2.90 ± 0.62 | – | 2.37 ± 0.57 | 0.52 ± 0.20 | LHCb [10] |
| 2.6 | 4.5 | 1.7 | – | QCD potential model [3] |
| 1.3 | 5.2 | 3.9 | – | QCD sum rules [4] |
| 2.0 | 5.7 | 2.9 | – | RCQM [5] |
| 2.2 | – | – | – | BSW [6] |
| 2.06 ± 0.86 | – | 3.01 ± 1.23 | – | LFQM [7] |
| $3.45^{+0.49}_{-0.17}$ | – | $2.54^{+0.07}_{-0.21}$ | 0.48 ± 0.04 | pQCD [8] |
| – | – | – | 0.410 | RIQM [9] |

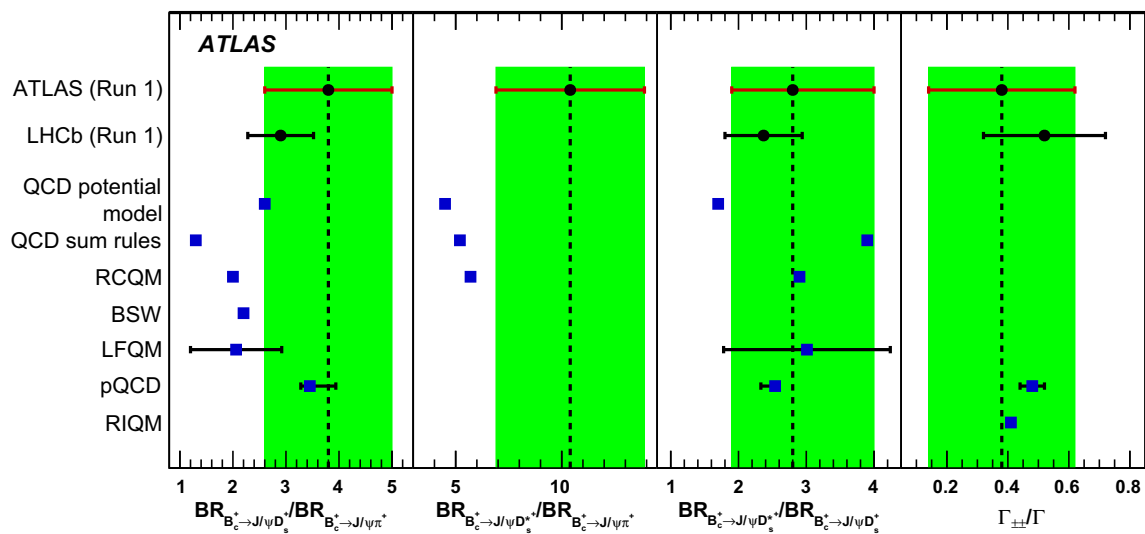


Fig. 7 Comparison of the results of this measurement with those of LHCb [10] and theoretical predictions based on a QCD relativistic potential model [3], QCD sum rules [4], relativistic constituent quark model (RCQM) [5], BSW relativistic quark model (with fixed average transverse quark momentum $\omega = 0.40\text{ GeV}$) [6], light-front quark

model (LFQM) [7], perturbative QCD (pQCD) [8], and relativistic independent quark model (RIQM) [9]. The uncertainties of the theoretical predictions are shown if they are explicitly quoted in the corresponding papers. Statistical and systematic uncertainties added in quadrature are quoted for the results of ATLAS and LHCb.

theoretical approaches. The measured ratios of the branching fraction are generally described by perturbative QCD, sum rules, and relativistic quark models. There is an indication of underestimation of the decay rates for the $B_c^+ \rightarrow J/\psi D_s^{(*)+}$ decays by some models, although the discrepancies do not exceed two standard deviations when taking into account only the experimental uncertainty. The measurement results agree with those published by the LHCb experiment.

Acknowledgments We thank CERN for the very successful operation of the LHC, as well as the support staff from our institutions without whom ATLAS could not be operated efficiently. We acknowledge the support of ANPCyT, Argentina; YerPhI, Armenia; ARC,

Australia; BMWFW and FWF, Austria; ANAS, Azerbaijan; SSTC, Belarus; CNPq and FAPESP, Brazil; NSERC, NRC and CFI, Canada; CERN; CONICYT, Chile; CAS, MOST and NSFC, China; COLCIENCIAS, Colombia; MSMT CR, MPO CR and VSC CR, Czech Republic; DNRF, DNSRC and Lundbeck Foundation, Denmark; EPLANET, ERC and NSRF, European Union; IN2P3-CNRS, CEA-DSM/IRFU, France; GNSF, Georgia; BMBF, DFG, HGF, MPG and AvH Foundation, Germany; GSRT and NSRF, Greece; RGC, Hong Kong SAR, China; ISF, MINERVA, GIF, I-CORE and Benozio Center, Israel; INFN, Italy; MEXT and JSPS, Japan; CNRST, Morocco; FOM and NWO, Netherlands; BRF and RCN, Norway; MNiSW and NCN, Poland; GRICES and FCT, Portugal; MNE/IFA, Romania; MES of Russia and NRC KI, Russian Federation; JINR; MSTP, Serbia; MSSR, Slovakia; ARRS and MIZŠ, Slovenia; DST/NRF, South Africa; MINECO, Spain; SRC and Wallenberg Foundation, Sweden; SER, SNSF and Cantons of Bern and

Geneva, Switzerland; NSC, Taiwan; TAEK, Turkey; STFC, the Royal Society and Leverhulme Trust, United Kingdom; DOE and NSF, United States of America. The crucial computing support from all WLCG partners is acknowledged gratefully, in particular from CERN and the ATLAS Tier-1 facilities at TRIUMF (Canada), NDGF (Denmark, Norway, Sweden), CC-IN2P3 (France), KIT/GridKA (Germany), INFN-CNAF (Italy), NL-T1 (Netherlands), PIC (Spain), ASGC (Taiwan), RAL (UK) and BNL (USA) and in the Tier-2 facilities worldwide.

Open Access This article is distributed under the terms of the Creative Commons Attribution 4.0 International License (<http://creativecommons.org/licenses/by/4.0/>), which permits unrestricted use, distribution, and reproduction in any medium, provided you give appropriate credit to the original author(s) and the source, provide a link to the Creative Commons license, and indicate if changes were made. Funded by SCOAP³.

References

1. CDF Collaboration, F. Abe et al., Phys. Rev. Lett. **81**, 2432–2437 (1998). [arXiv:hep-ex/9805034](https://arxiv.org/abs/hep-ex/9805034). doi:10.1103/PhysRevLett.81.2432
2. ATLAS Collaboration, Phys. Rev. Lett. **113**, 212004 (2014). [arXiv:1407.1032](https://arxiv.org/abs/1407.1032) [hep-ex]. doi:10.1103/PhysRevLett.113.212004
3. P. Colangelo, F. De Fazio, Phys. Rev. D **61**, 034012 (2000). doi:10.1103/PhysRevD.61.034012. [arXiv:hep-ph/9909423](https://arxiv.org/abs/hep-ph/9909423)
4. V. Kiselev, Exclusive decays and lifetime of B_c meson in QCD sum rules (2002). [arXiv:hep-ph/0211021](https://arxiv.org/abs/hep-ph/0211021) [hep-ph]
5. M. Ivanov, J. Korner, P. Santorelli, Phys. Rev. D **73**, 054024 (2006). doi:10.1103/PhysRevD.73.054024. [arXiv:hep-ph/0602050](https://arxiv.org/abs/hep-ph/0602050)
6. R. Dhir, R. Verma, Phys. Rev. D **79**, 034004 (2009). doi:10.1103/PhysRevD.79.034004. [arXiv:0810.4284](https://arxiv.org/abs/0810.4284) [hep-ph]
7. H.-W. Ke, T. Liu, X.-Q. Li, Phys. Rev. D **89**, 017501 (2014). doi:10.1103/PhysRevD.89.017501. [arXiv:1307.5925](https://arxiv.org/abs/1307.5925) [hep-ph]
8. Z. Rui, Z.-T. Zou, Phys. Rev. D **90**, 114030 (2014). doi:10.1103/PhysRevD.90.114030. [arXiv:1407.5550](https://arxiv.org/abs/1407.5550) [hep-ph]
9. S. Kar et al., Phys. Rev. D **88**, 094014 (2013). doi:10.1103/PhysRevD.88.094014
10. LHCb Collaboration, R. Aaij et al., Phys. Rev. D **87**, 112012 (2013). [arXiv:1304.4530](https://arxiv.org/abs/1304.4530) [hep-ex]. doi:10.1103/PhysRevD.87.112012
11. ATLAS Collaboration, JINST **3**, S08003 (2008). doi:10.1088/1748-0221/3/08/S08003
12. T. Sjostrand, S. Mrenna, P. Skands, JHEP **0605**, 026 (2006). [arXiv:hep-ph/0603175](https://arxiv.org/abs/hep-ph/0603175). doi:10.1088/1126-6708/2006/05/026
13. A. Berezhnoy, A. Likhoded and O. Yushchenko, Phys. Atom. Nucl. **59** (1996) 709–713. [arXiv:hep-ph/9504302](https://arxiv.org/abs/hep-ph/9504302) [hep-ph]
14. A. Berezhnoy, V. Kiselev, A. Likhoded, Z. Phys. A **356**, 79–87 (1996). [arXiv:hep-ph/9602347](https://arxiv.org/abs/hep-ph/9602347). doi:10.1007/s002180050151
15. A. Berezhnoy et al., Phys. Atom. Nucl. **60** (1997) 1729–1740. [arXiv:hep-ph/9703341](https://arxiv.org/abs/hep-ph/9703341) [hep-ph]
16. A. Berezhnoy, Phys. Atom. Nucl. **68**, 1866–1872 (2005). [arXiv:hep-ph/0407315](https://arxiv.org/abs/hep-ph/0407315). doi:10.1134/1.2131116
17. D. Lange, Nucl. Instrum. Meth. A **462**, 152–155 (2001). doi:10.1016/S0168-9002(01)00089-4
18. ATLAS Collaboration, Eur. Phys. J. C **70**, 823–874 (2010). [arXiv:1005.4568](https://arxiv.org/abs/1005.4568) [physics.ins-det]. doi:10.1140/epjc/s10052-010-1429-9
19. GEANT4 Collaboration, S. Agostinelli et al., Nucl. Instrum. Meth. A **506**, 250–303 (2003). doi:10.1016/S0168-9002(03)01368-8
20. J. Allison et al., IEEE Trans. Nucl. Sci. **53**, 270 (2006). doi:10.1109/TNS.2006.869826
21. V. Kostyukhin, VKalVrt - package for vertex reconstruction in ATLAS, ATL-PHYS-2003-031 (2003). <http://cds.cern.ch/record/685551>
22. K. A. Olive et al., Particle Data Group, Chin. Phys. C **38**, 090001 (2014). doi:10.1088/1674-1137/38/9/090001
23. ZEUS Collaboration, S. Chekanov et al., Eur. Phys. J. C **44**, 13–25 (2005). [arXiv:hep-ex/0505008](https://arxiv.org/abs/hep-ex/0505008). doi:10.1140/epjc/s2005-02346-2
24. G. Aad et al., Nucl. Phys. B **864**, 341–381 (2012). [arXiv:1206.3122](https://arxiv.org/abs/1206.3122) [hep-ex]. doi:10.1016/j.nuclphysb.2012.07.009
25. K. Cranmer, Comput. Phys. Commun. **136**, 198–207 (2001). [arXiv:hep-ex/0011057](https://arxiv.org/abs/hep-ex/0011057) [hep-ex]. doi:10.1016/S0010-4655(00)00243-5
26. CLEO Collaboration, J. Alexander et al., Phys. Rev. Lett. **100**, 161804 (2008). doi:10.1103/PhysRevLett.100.161804. [arXiv:0801.0680](https://arxiv.org/abs/0801.0680) [hep-ex]
27. M. Oreglia, A study of the reactions $\psi' \rightarrow \gamma\gamma\psi$, PhD thesis, Stanford University, SLAC-R-236 (1980). <http://www.slac.stanford.edu/pubs/slacreports/slac-r-236.html>
28. J. Gaiser, Charmonium spectroscopy from radiative decays of the J/ψ and ψ' , PhD thesis, Stanford University, SLAC-R-255 (1982). <http://www.slac.stanford.edu/pubs/slacreports/slac-r-255.html>
29. T. Skwarnicki, A study of the radiative cascade transitions between the Υ' and Υ resonances, PhD thesis, Institute of Nuclear Physics, Krakow, DESY-F31-86-02 (1986). <http://inspirehep.net/record/230779/>

ATLAS Collaboration

G. Aad⁸⁵, B. Abbott¹¹³, J. Abdallah¹⁵¹, O. Abdinov¹¹, R. Aben¹⁰⁷, M. Abolins⁹⁰, O. S. AbouZeid¹⁵⁸, H. Abramowicz¹⁵³, H. Abreu¹⁵², R. Abreu³⁰, Y. Abulaiti^{146a,146b}, B. S. Acharya^{164a,164b,a}, L. Adamczyk^{38a}, D. L. Adams²⁵, J. Adelman¹⁰⁸, S. Adomeit¹⁰⁰, T. Adye¹³¹, A. A. Affolder⁷⁴, T. Agatonovic-Jovin¹³, J. A. Aguilar-Saavedra^{126a,126f}, S. P. Ahlen²², F. Ahmadov^{65,b}, G. Aielli^{133a,133b}, H. Akerstedt^{146a,146b}, T. P. A. Åkesson⁸¹, G. Akimoto¹⁵⁵, A. V. Akimov⁹⁶, G. L. Alberghi^{20a,20b}, J. Albert¹⁶⁹, S. Albrand⁵⁵, M. J. Alconada Verzini⁷¹, M. Aleksa³⁰, I. N. Aleksandrov⁶⁵, C. Alexa^{26a}, G. Alexander¹⁵³, T. Alexopoulos¹⁰, M. Alhroob¹¹³, G. Alimonti^{91a}, L. Alio⁸⁵, J. Alison³¹, S. P. Alkire³⁵, B. M. M. Allbrooke¹⁸, P. P. Allport⁷⁴, A. Aloisio^{104a,104b}, A. Alonso³⁶, F. Alonso⁷¹, C. Alpigiani⁷⁶, A. Altheimer³⁵, B. Alvarez Gonzalez³⁰, D. Álvarez Piqueras¹⁶⁷, M. G. Alvigi^{104a,104b}, B. T. Amadio¹⁵, K. Amako⁶⁶, Y. Amaral Coutinho^{24a}, C. Amelung²³, D. Amidei⁸⁹, S. P. Amor Dos Santos^{126a,126c}, A. Amorim^{126a,126b}, S. Amoroso⁴⁸, N. Amram¹⁵³, G. Amundsen²³, C. Anastopoulos¹³⁹, L. S. Ancu⁴⁹, N. Andari³⁰, T. Andeen³⁵, C. F. Anders^{58b}, G. Anders³⁰, J. K. Anders⁷⁴, K. J. Anderson³¹, A. Andreazza^{91a,91b}, V. Andrei^{58a}, S. Angelidakis⁹, I. Angelozzi¹⁰⁷, P. Anger⁴⁴, A. Angerami³⁵, F. Anghinolfi³⁰, A. V. Anisenkov^{109,c}, N. Anjos¹², A. Annovi^{124a,124b}, M. Antonelli⁴⁷, A. Antonov⁹⁸, J. Antos^{144b}, F. Anulli^{132a}, M. Aoki⁶⁶, L. Aperio Bella¹⁸, G. Arabidze⁹⁰, Y. Arai⁶⁶, J. P. Araque^{126a}, A. T. H. Arce⁴⁵, F. A. Arduh⁷¹, J.-F. Arguin⁹⁵, S. Argyropoulos⁴², M. Arik^{19a}, A. J. Armbruster³⁰, O. Arnaez³⁰, V. Arnal⁸², H. Arnold⁴⁸, M. Arratia²⁸, O. Arslan²¹, A. Artamonov⁹⁷, G. Artoni²³, S. Asai¹⁵⁵, N. Asbah⁴², A. Ashkenazi¹⁵³, B. Åsman^{146a,146b}, L. Asquith¹⁴⁹, K. Assamagan²⁵, R. Astalos^{144a}, M. Atkinson¹⁶⁵, N. B. Atlay¹⁴¹, B. Auerbach⁶, K. Augsten¹²⁸, M. Aurousseau^{145b}, G. Avolio³⁰, B. Axen¹⁵, M. K. Ayoub¹¹⁷, G. Azuelos^{95,d}, M. A. Baak³⁰, A. E. Baas^{58a}, C. Bacci^{134a,134b}, H. Bachacou¹³⁶, K. Bachas¹⁵⁴, M. Backes³⁰, M. Backhaus³⁰, P. Bagiacchi^{132a,132b}, P. Bagnaia^{132a,132b}, Y. Bai^{33a}, T. Bain³⁵, J. T. Baines¹³¹, O. K. Baker¹⁷⁶, P. Balek¹²⁹, T. Balestri¹⁴⁸, F. Balli⁸⁴, E. Banas³⁹, Sw. Banerjee¹⁷³, A. A. E. Bannoura¹⁷⁵, H. S. Bansil¹⁸, L. Barak³⁰, E. L. Barberio⁸⁸, D. Barberis^{50a,50b}, M. Barbero⁸⁵, T. Barillari¹⁰¹, M. Barisonzi^{164a,164b}, T. Barklow¹⁴³, N. Barlow²⁸, S. L. Barnes⁸⁴, B. M. Barnett¹³¹, R. M. Barnett¹⁵, Z. Barnovska⁵, A. Baroncelli^{134a}, G. Barone⁴⁹, A. J. Barr¹²⁰, F. Barreiro⁸², J. Barreiro Guimarães da Costa⁵⁷, R. Bartoldus¹⁴³, A. E. Barton⁷², P. Bartos^{144a}, A. Basalae¹²³, A. Bassalat¹¹⁷, A. Basye¹⁶⁵, R. L. Bates⁵³, S. J. Batista¹⁵⁸, J. R. Batley²⁸, M. Battaglia¹³⁷, M. Bause^{132a,132b}, F. Bauer¹³⁶, H. S. Bawa^{143,e}, J. B. Beacham¹¹¹, M. D. Beattie⁷², T. Beau⁸⁰, P. H. Beauchemin¹⁶¹, R. Beccherle^{124a,124b}, P. Bechtel²¹, H. P. Beck^{17,f}, K. Becker¹²⁰, M. Becker⁸³, S. Becker¹⁰⁰, M. Beckingham¹⁷⁰, C. Becot¹¹⁷, A. J. Beddall^{19b}, A. Beddall^{19b}, V. A. Bednyakov⁶⁵, C. P. Bee¹⁴⁸, L. J. Beemster¹⁰⁷, T. A. Beermann¹⁷⁵, M. Begel²⁵, J. K. Behr¹²⁰, C. Belanger-Champagne⁸⁷, W. H. Bell⁴⁹, G. Bella¹⁵³, L. Bellagamba^{20a}, A. Bellerive²⁹, M. Bellomo⁸⁶, K. Belotskiy⁹⁸, O. Beltramello³⁰, O. Benary¹⁵³, D. Benchechroun^{135a}, M. Bender¹⁰⁰, K. Bendtz^{146a,146b}, N. Benekos¹⁰, Y. Benhammou¹⁵³, E. Benhar Nocchioli⁴⁹, J. A. Benítez García^{159b}, D. P. Benjamin⁴⁵, J. R. Bensinger²³, S. Bentvelsen¹⁰⁷, L. Beresford¹²⁰, M. Beretta⁴⁷, D. Berge¹⁰⁷, E. Bergeaas Kuutmann¹⁶⁶, N. Berger⁵, F. Berghaus¹⁶⁹, J. Beringer¹⁵, C. Bernard²², N. R. Bernard⁸⁶, C. Bernius¹¹⁰, F. U. Bernlochner²¹, T. Berry⁷⁷, P. Berta¹²⁹, C. Bertella⁸³, G. Bertoli^{146a,146b}, F. Bertolucci^{124a,124b}, C. Bertsche¹¹³, D. Bertsche¹¹³, M. I. Besana^{91a}, G. J. Besjes¹⁰⁶, O. Bessidskaia Bylund^{146a,146b}, M. Bessner⁴², N. Besson¹³⁶, C. Betancourt⁴⁸, S. Bethke¹⁰¹, A. J. Bevan⁷⁶, W. Bhimji⁴⁶, R. M. Bianchi¹²⁵, L. Bianchini²³, M. Bianco³⁰, O. Biebel¹⁰⁰, S. P. Bieniek⁷⁸, M. Biglietti^{134a}, J. Bilbao De Mendizabal⁴⁹, H. Bilokon⁴⁷, M. Bindi⁵⁴, S. Binet¹¹⁷, A. Bingul^{19b}, C. Bini^{132a,132b}, C. W. Black¹⁵⁰, J. E. Black¹⁴³, K. M. Black²², D. Blackburn¹³⁸, R. E. Blair⁶, J.-B. Blanchard¹³⁶, J. E. Blanco⁷⁷, T. Blazek^{144a}, I. Bloch⁴², C. Blocker²³, W. Blum^{83,*}, U. Blumenschein⁵⁴, G. J. Bobbink¹⁰⁷, V. S. Bobrovnikov^{109,c}, S. S. Bocchetta⁸¹, A. Bocchi⁴⁵, C. Bock¹⁰⁰, M. Boehler⁴⁸, J. A. Bogaerts³⁰, D. Bogavac¹³, A. G. Bogdanchikov¹⁰⁹, C. Bohm^{146a}, V. Boisvert⁷⁷, T. Bold^{38a}, V. Boldea^{26a}, A. S. Boldyrev⁹⁹, M. Bomben⁸⁰, M. Bona⁷⁶, M. Boonekamp¹³⁶, A. Borisov¹³⁰, G. Borissov⁷², S. Borroni⁴², J. Bortfeldt¹⁰⁰, V. Bortolotto^{60a,60b,60c}, K. Bos¹⁰⁷, D. Boscherini^{20a}, M. Bosman¹², J. Boudreau¹²⁵, J. Bouffard², E. V. Bouhova-Thacker⁷², D. Boumediene³⁴, C. Bourdarios¹¹⁷, N. Bousson¹¹⁴, A. Boveia³⁰, J. Boyd³⁰, I. R. Boyko⁶⁵, I. Bozic¹³, J. Bracinik¹⁸, A. Brandt⁸, G. Brandt⁵⁴, O. Brandt^{58a}, U. Bratzler¹⁵⁶, B. Brau⁸⁶, J. E. Brau¹¹⁶, H. M. Braun^{175,*}, S. F. Brazzale^{164a,164c}, W. D. Breaden Madden⁵³, K. Brendlinger¹²², A. J. Brennan⁸⁸, L. Brenner¹⁰⁷, R. Brenner¹⁶⁶, S. Bressler¹⁷², K. Bristow^{145c}, T. M. Bristow⁴⁶, D. Britton⁵³, D. Britzger⁴², F. M. Brochu²⁸, I. Brock²¹, R. Brock⁹⁰, J. Bronner¹⁰¹, G. Brooijmans³⁵, T. Brooks⁷⁷, W. K. Brooks^{32b}, J. Brosamer¹⁵, E. Brost¹¹⁶, J. Brown⁵⁵, P. A. Bruckman de Renstrom³⁹, D. Bruncko^{144b}, R. Bruneliere⁴⁸, A. Bruni^{20a}, G. Bruni^{20a}, M. Bruschi^{20a}, N. Bruscino²¹, L. Bryngemark⁸¹, T. Buanes¹⁴, Q. Buat¹⁴², P. Buchholz¹⁴¹, A. G. Buckley⁵³, S. I. Buda^{26a}, I. A. Budagov⁶⁵, F. Buehrer⁴⁸, L. Bugge¹¹⁹, M. K. Bugge¹¹⁹, O. Bulekov⁹⁸, D. Bullock⁸, H. Burckhart³⁰, S. Burdin⁷⁴, B. Burghgrave¹⁰⁸, S. Burke¹³¹, I. Burmeister⁴³, E. Busato³⁴, D. Büscher⁴⁸, V. Büscher⁸³, P. Bussey⁵³, J. M. Butler²², A. I. Butt³, C. M. Buttar⁵³, J. M. Butterworth⁷⁸, P. Butti¹⁰⁷, W. Buttinger²⁵, A. Buzatu⁵³, A. R. Buzykaev^{109,c}, S. Cabrera Urbán¹⁶⁷, D. Caforio¹²⁸, V. M. Cairo^{37a,37b}, O. Cakir^{4a}, P. Calafiura¹⁵, A. Calandri¹³⁶, G. Calderini⁸⁰, P. Calfayan¹⁰⁰, L. P. Caloba^{24a}, D. Calvet³⁴, S. Calvet³⁴, R. Camacho Toro³¹,

S. Camarda⁴², P. Camarri^{133a,133b}, D. Cameron¹¹⁹, L. M. Caminada¹⁵, R. Caminal Armadans¹⁶⁵, S. Campana³⁰, M. Campanelli⁷⁸, A. Campoverde¹⁴⁸, V. Canale^{104a,104b}, A. Canepa^{159a}, M. Cano Bret⁷⁶, J. Cantero⁸², R. Cantrill^{126a}, T. Cao⁴⁰, M. D. M. Capeans Garrido³⁰, I. Caprini^{26a}, M. Caprini^{26a}, M. Capua^{37a,37b}, R. Caputo⁸³, R. Cardarelli^{133a}, F. Cardillo⁴⁸, T. Carli³⁰, G. Carlino^{104a}, L. Carminati^{91a,91b}, S. Caron¹⁰⁶, E. Carquin^{32a}, G. D. Carrillo-Montoya⁸, J. R. Carter²⁸, J. Carvalho^{126a,126c}, D. Casadei⁷⁸, M. P. Casado¹², M. Casolino¹², E. Castaneda-Miranda^{145b}, A. Castelli¹⁰⁷, V. Castillo Gimenez¹⁶⁷, N. F. Castro^{126a,g}, P. Catastini⁵⁷, A. Catinaccio³⁰, J. R. Catmore¹¹⁹, A. Cattai³⁰, J. Caudron⁸³, V. Cavaliere¹⁶⁵, D. Cavalli^{91a}, M. Cavalli-Sforza¹², V. Cavalinni^{124a,124b}, F. Ceradini^{134a,134b}, B. C. Cerio⁴⁵, K. Cerny¹²⁹, A. S. Cerqueira^{24b}, A. Cerri¹⁴⁹, L. Cerrito⁷⁶, F. Cerutti¹⁵, M. Cerv³⁰, A. Cervelli¹⁷, S. A. Cetin^{19c}, A. Chafaq^{135a}, D. Chakraborty¹⁰⁸, I. Chalupkova¹²⁹, P. Chang¹⁶⁵, B. Chapleau⁸⁷, J. D. Chapman²⁸, D. G. Charlton¹⁸, C. C. Chau¹⁵⁸, C. A. Chavez Barajas¹⁴⁹, S. Cheatham¹⁵², A. Chegwidan⁹⁰, S. Chekanov⁶, S. V. Chekulaev^{159a}, G. A. Chelkov^{65,h}, M. A. Chelstowska⁸⁹, C. Chen⁶⁴, H. Chen²⁵, K. Chen¹⁴⁸, L. Chen^{33d,i}, S. Chen^{33c}, X. Chen^{33f}, Y. Chen⁶⁷, H. C. Cheng⁸⁹, Y. Cheng³¹, A. Cheplakov⁶⁵, E. Cheremushkina¹³⁰, R. Cherkaoui El Moursli^{135e}, V. Chernyatin^{25,*}, E. Cheu⁷, L. Chevalier¹³⁶, V. Chiarella⁴⁷, J. T. Childers⁶, G. Chiodini^{73a}, A. S. Chisholm¹⁸, R. T. Chislett⁷⁸, A. Chitan^{26a}, M. V. Chizhov⁶⁵, K. Choi⁶¹, S. Chouridou⁹, B. K. B. Chow¹⁰⁰, V. Christodoulou⁷⁸, D. Chromek-Burckhart³⁰, J. Chudoba¹²⁷, A. J. Chuinard⁸⁷, J. J. Chwastowski³⁹, L. Chytka¹¹⁵, G. Ciapetti^{132a,132b}, A. K. Ciftci^{4a}, D. Cincă⁵³, V. Cindro⁷⁵, I. A. Cioara²¹, A. Ciocio¹⁵, Z. H. Citron¹⁷², M. Ciubancan^{26a}, A. Clark⁴⁹, B. L. Clark⁵⁷, P. J. Clark⁴⁶, R. N. Clarke¹⁵, W. Cleland¹²⁵, C. Clement^{146a,146b}, Y. Coadou⁸⁵, M. Cobal^{164a,164c}, A. Cocco¹³⁸, J. Cochran⁶⁴, L. Coffey²³, J. G. Cogan¹⁴³, B. Cole³⁵, S. Cole¹⁰⁸, A. P. Colijn¹⁰⁷, J. Collot⁵⁵, T. Colombo^{58c}, G. Compostella¹⁰¹, P. Conde Muñio^{126a,126b}, E. Coniavitis⁴⁸, S. H. Connell^{145b}, I. A. Connelly⁷⁷, S. M. Consonni^{91a,91b}, V. Consorti⁴⁸, S. Constantinescu^{26a}, C. Conta^{121a,121b}, G. Conti³⁰, F. Conventi^{104a,j}, M. Cooke¹⁵, B. D. Cooper⁷⁸, A. M. Cooper-Sarkar¹²⁰, T. Cornelissen¹⁷⁵, M. Corradi^{20a}, F. Corriveau^{87,k}, A. Corso-Radu¹⁶³, A. Cortes-Gonzalez¹², G. Cortiana¹⁰¹, G. Costa^{91a}, M. J. Costa¹⁶⁷, D. Costanzo¹³⁹, D. Côté⁸, G. Cottin²⁸, G. Cowan⁷⁷, B. E. Cox⁸⁴, K. Cranmer¹¹⁰, G. Cree²⁹, S. Crépe-Renaudin⁵⁵, F. Crescioli⁸⁰, W. A. Cribbs^{146a,146b}, M. Crispin Ortuzar¹²⁰, M. Cristinziani²¹, V. Croft¹⁰⁶, G. Crosetti^{37a,37b}, T. Cuhadar Donszelmann¹³⁹, J. Cummings¹⁷⁶, M. Curatolo⁴⁷, C. Cuthbert¹⁵⁰, H. Czir¹⁴¹, P. Czodrowski³, S. D'Auria⁵³, M. D'Onofrio⁷⁴, M. J. Da Cunha Sargedas De Sousa^{126a,126b}, C. Da Via⁸⁴, W. Dabrowski^{38a}, A. Dafinca¹²⁰, T. Dai⁸⁹, O. Dale¹⁴, F. Dallaire⁹⁵, C. Dallapiccola⁸⁶, M. Dam³⁶, J. R. Dandoy³¹, N. P. Dang⁴⁸, A. C. Daniells¹⁸, M. Danninger¹⁶⁸, M. Dano Hoffmann¹³⁶, V. Dao⁴⁸, G. Darbo^{50a}, S. Darmora⁸, J. Dassoulas³, A. Dattagupta⁶¹, W. Davey²¹, C. David¹⁶⁹, T. Davidek¹²⁹, E. Davies^{120,l}, M. Davies¹⁵³, P. Davison⁷⁸, Y. Davygora^{58a}, E. Dawe⁸⁸, I. Dawson¹³⁹, R. K. Daya-Ishmukhametova⁸⁶, K. De⁸, R. de Asmundis^{104a}, S. De Castro^{20a,20b}, S. De Cecco⁸⁰, N. De Groot¹⁰⁶, P. de Jong¹⁰⁷, H. De la Torre⁸², F. De Lorenzi⁶⁴, L. De Nooij¹⁰⁷, D. De Pedis^{132a}, A. De Salvo^{132a}, U. De Sanctis¹⁴⁹, A. De Santo¹⁴⁹, J. B. De Vivie De Regie¹¹⁷, W. J. Dearnaley⁷², R. Debbé²⁵, C. Debenedetti¹³⁷, D. V. Dedovich⁶⁵, I. Deigaard¹⁰⁷, J. Del Peso⁸², T. Del Prete^{124a,124b}, D. Delgove¹¹⁷, F. Deliot¹³⁶, C. M. Delitzsch⁴⁹, M. Deliyergiyev⁷⁵, A. Dell'Acqua³⁰, L. Dell'Asta²², M. Dell'Orso^{124a,124b}, M. Della Pietra^{104a,j}, D. della Volpe⁴⁹, M. Delmastro⁵, P. A. Delsart⁵⁵, C. Deluca¹⁰⁷, D. A. DeMarco¹⁵⁸, S. Demers¹⁷⁶, M. Demichev⁶⁵, A. Demilly⁸⁰, S. P. Denisov¹³⁰, D. Derendarz³⁹, J. E. Derkaoui^{135d}, F. Derue⁸⁰, P. Dervan⁷⁴, K. Desch²¹, C. Deterre⁴², P. O. Deviveiros³⁰, A. Dewhurst¹³¹, S. Dhaliwal²³, A. Di Ciaccio^{133a,133b}, L. Di Ciaccio⁵, A. Di Domenico^{132a,132b}, C. Di Donato^{104a,104b}, A. Di Girolamo³⁰, B. Di Girolamo³⁰, A. Di Mattia¹⁵², B. Di Micco^{134a,134b}, R. Di Nardo⁴⁷, A. Di Simone⁴⁸, R. Di Sipio¹⁵⁸, D. Di Valentino²⁹, C. Diaconu⁸⁵, M. Diamond¹⁵⁸, F. A. Dias⁴⁶, M. A. Diaz^{32a}, E. B. Diehl⁸⁹, J. Dietrich¹⁶, S. Diglio⁸⁵, A. Dimitrievska¹³, J. Dingfelder²¹, P. Dita^{26a}, S. Dita^{26a}, F. Dittus³⁰, F. Djama⁸⁵, T. Djobava^{51b}, J. I. Djuvsland^{58a}, M. A. B. do Vale^{24c}, D. Dobos³⁰, M. Dobre^{26a}, C. Doglioni⁴⁹, T. Dohmae¹⁵⁵, J. Dolejsi¹²⁹, Z. Dolezal¹²⁹, B. A. Dolgoshein^{98,*}, M. Donadelli^{24d}, S. Donati^{124a,124b}, P. Dondero^{121a,121b}, J. Donini³⁴, J. Dopke¹³¹, A. Doria^{104a}, M. T. Dova⁷¹, A. T. Doyle⁵³, E. Drechsler⁵⁴, M. Dris¹⁰, E. Dubreuil³⁴, E. Duchovni¹⁷², G. Duckeck¹⁰⁰, O. A. Ducu^{26a,85}, D. Duda¹⁷⁵, A. Dudarev³⁰, L. Dufloc¹¹⁷, L. Duguid⁷⁷, M. Dührssen³⁰, M. Dunford^{58a}, H. Duran Yildiz^{4a}, M. Düren⁵², A. Durglishvili^{51b}, D. Duschinger⁴⁴, M. Dyndal^{38a}, C. Eckardt⁴², K. M. Ecker¹⁰¹, R. C. Edgar⁸⁹, W. Edson², N. C. Edwards⁴⁶, W. Ehrenfeld²¹, T. Eifert³⁰, G. Eigen¹⁴, K. Einsweiler¹⁵, T. Ekelof¹⁶⁶, M. El Kacimi^{135c}, M. Ellert¹⁶⁶, S. Elles⁵, F. Ellinghaus⁸³, A. A. Elliot¹⁶⁹, N. Ellis³⁰, J. Elmsheuser¹⁰⁰, M. Elsing³⁰, D. Emeliyanov¹³¹, Y. Enari¹⁵⁵, O. C. Endner⁸³, M. Endo¹¹⁸, J. Erdmann⁴³, A. Ereditato¹⁷, G. Ernis¹⁷⁵, J. Ernst², M. Ernst²⁵, S. Errede¹⁶⁵, E. Ertel⁸³, M. Escalier¹¹⁷, H. Esch⁴³, C. Escobar¹²⁵, B. Esposito⁴⁷, A. I. Etienne¹³⁶, E. Etzion¹⁵³, H. Evans⁶¹, A. Ezhilov¹²³, L. Fabbri^{20a,20b}, G. Facini³¹, R. M. Fakhruddinov¹³⁰, S. Falciano^{132a}, R. J. Falla⁷⁸, J. Faltova¹²⁹, Y. Fang^{33a}, M. Fanti^{91a,91b}, A. Farbin⁸, A. Farilla^{134a}, T. Farooque¹², S. Farrell¹⁵, S. M. Farrington¹⁷⁰, P. Farthouat³⁰, F. Fassi^{135e}, P. Fassnacht³⁰, D. Fassouliotis⁹, M. Fauci Giannelli⁷⁷, A. Favareto^{50a,50b}, L. Fayard¹¹⁷, P. Federic^{144a}, O. L. Fedin^{123,m}, W. Fedorko¹⁶⁸, S. Feigl³⁰, L. Felgioni⁸⁵, C. Feng^{33d}, E. J. Feng⁶, H. Feng⁸⁹, A. B. Fenyuk¹³⁰, L. Feremenga⁸, P. Fernandez Martinez¹⁶⁷, S. Fernandez Perez³⁰, J. Ferrando⁵³, A. Ferrari¹⁶⁶, P. Ferrari¹⁰⁷,

R. Ferrari^{121a}, D. E. Ferreira de Lima⁵³, A. Ferrer¹⁶⁷, D. Ferrere⁴⁹, C. Ferretti⁸⁹, A. Ferretto Parodi^{50a,50b}, M. Fiascaris³¹, F. Fiedler⁸³, A. Filipčić⁷⁵, M. Filipuzzi⁴², F. Filthaut¹⁰⁶, M. Fincke-Keeler¹⁶⁹, K. D. Finelli¹⁵⁰, M. C. N. Fiolhais^{126a,126c}, L. Fiorini¹⁶⁷, A. Firan⁴⁰, A. Fischer², C. Fischer¹², J. Fischer¹⁷⁵, W. C. Fisher⁹⁰, E. A. Fitzgerald²³, I. Fleck¹⁴¹, P. Fleischmann⁸⁹, S. Fleischmann¹⁷⁵, G. T. Fletcher¹³⁹, G. Fletcher⁷⁶, R. R. M. Fletcher¹²², T. Flick¹⁷⁵, A. Floderus⁸¹, L. R. Flores Castillo^{60a}, M. J. Flowerdew¹⁰¹, A. Formica¹³⁶, A. Forti⁸⁴, D. Fournier¹¹⁷, H. Fox⁷², S. Fracchia¹², P. Francavilla⁸⁰, M. Franchini^{20a,20b}, D. Francis³⁰, L. Franconi¹¹⁹, M. Franklin⁵⁷, M. Frate¹⁶³, M. Fraternali^{121a,121b}, D. Freeborn⁷⁸, S. T. French²⁸, F. Friedrich⁴⁴, D. Froidevaux³⁰, J. A. Frost¹²⁰, C. Fukunaga¹⁵⁶, E. Fullana Torregrosa⁸³, B. G. Fulson¹⁴³, J. Fuster¹⁶⁷, C. Gabaldon⁵⁵, O. Gabizon¹⁷⁵, A. Gabrielli^{20a,20b}, A. Gabrielli^{132a,132b}, S. Gadatsch¹⁰⁷, S. Gadomski⁴⁹, G. Gagliardi^{50a,50b}, P. Gagnon⁶¹, C. Galea¹⁰⁶, B. Galhardo^{126a,126c}, E. J. Gallas¹²⁰, B. J. Gallop¹³¹, P. Gallus¹²⁸, G. Galster³⁶, K. K. Gan¹¹¹, J. Gao^{33b,85}, Y. Gao⁴⁶, Y. S. Gao^{143,e}, F. M. Garay Walls⁴⁶, F. Garberson¹⁷⁶, C. García¹⁶⁷, J. E. García Navarro¹⁶⁷, M. Garcia-Sciveres¹⁵, R. W. Gardner³¹, N. Garelli¹⁴³, V. Garonne¹¹⁹, C. Gatti⁴⁷, A. Gaudiello^{50a,50b}, G. Gaudio^{121a}, B. Gaur¹⁴¹, L. Gauthier⁹⁵, P. Gauzzi^{132a,132b}, I. L. Gavrilenko⁹⁶, C. Gay¹⁶⁸, G. Gaycken²¹, E. N. Gazis¹⁰, P. Ge^{33d}, Z. Gece¹⁶⁸, C. N. P. Gee¹³¹, D. A. A. Geerts¹⁰⁷, Ch. Geich-Gimbel²¹, M. P. Geisler^{58a}, C. Gemme^{50a}, M. H. Genest⁵⁵, S. Gentile^{132a,132b}, M. George⁵⁴, S. George⁷⁷, D. Gerbaudo¹⁶³, A. Gershon¹⁵³, H. Ghazlane^{135b}, B. Giacobbe^{20a}, S. Giagu^{132a,132b}, V. Giangiobbe¹², P. Giannetti^{124a,124b}, B. Gibbard²⁵, S. M. Gibson⁷⁷, M. Gilchriese¹⁵, T. P. S. Gillam²⁸, D. Gillberg³⁰, G. Gilles³⁴, D. M. Gingrich^{3,d}, N. Giokaris⁹, M. P. Giordani^{164a,164c}, F. M. Giorgi^{20a}, F. M. Giorgi¹⁶, P. F. Giraud¹³⁶, P. Giromini⁴⁷, D. Giugni^{91a}, C. Giuliani⁴⁸, M. Giulini^{58b}, B. K. Gjelsten¹¹⁹, S. Gkaitatzis¹⁵⁴, I. Gkialas¹⁵⁴, E. L. Gkougkousis¹¹⁷, L. K. Gladilin⁹⁹, C. Glasman⁸², J. Glatzer³⁰, P. C. F. Glaysher⁴⁶, A. Glazov⁴², M. Goblirsch-Kolb¹⁰¹, J. R. Goddard⁷⁶, J. Godlewski³⁹, S. Goldfarb⁸⁹, T. Golling⁴⁹, D. Golubkov¹³⁰, A. Gomes^{126a,126b,126d}, R. Gonçalves^{126a}, J. Goncalves Pinto Firmino Da Costa¹³⁶, L. Gonella²¹, S. González de la Hoz¹⁶⁷, G. Gonzalez Parra¹², S. Gonzalez-Sevilla⁴⁹, L. Goossens³⁰, P. A. Gorbounov⁹⁷, H. A. Gordon²⁵, I. Gorelov¹⁰⁵, B. Gorini³⁰, E. Gorini^{73a,73b}, A. Gorišek⁷⁵, E. Gornicki³⁹, A. T. Goshaw⁴⁵, C. Gössling⁴³, M. I. Gostkin⁶⁵, D. Goujdami^{135c}, A. G. Goussiou¹³⁸, N. Govender^{145b}, E. Gozani¹⁵², H. M. X. Grabas¹³⁷, L. Graber⁵⁴, I. Grabowska-Bold^{38a}, P. Grafström^{20a,20b}, K.-J. Grahm⁴², J. Gramling⁴⁹, E. Gramstad¹¹⁹, S. Grancagnolo¹⁶, V. Grassi¹⁴⁸, V. Gratchev¹²³, H. M. Gray³⁰, E. Graziani^{134a}, Z. D. Greenwood^{79,n}, K. Gregersen⁷⁸, I. M. Gregor⁴², P. Grenier¹⁴³, J. Griffiths⁸, A. A. Grillo¹³⁷, K. Grimm⁷², S. Grinstein^{12,o}, Ph. Gris³⁴, J.-F. Grivaz¹¹⁷, J. P. Grohs⁴⁴, A. Grohsjean⁴², E. Gross¹⁷², J. Grosse-Knetter⁵⁴, G. C. Grossi⁷⁹, Z. J. Grout¹⁴⁹, L. Guan^{33b}, J. Guenther¹²⁸, F. Guescini⁴⁹, D. Guest¹⁷⁶, O. Gueta¹⁵³, E. Guido^{50a,50b}, T. Guillemin¹¹⁷, S. Guindon², U. Gul⁵³, C. Gumpert⁴⁴, J. Guo^{33e}, S. Gupta¹²⁰, G. Gustavino^{132a,132b}, P. Gutierrez¹¹³, N. G. Gutierrez Ortiz⁵³, C. Gutsche⁴⁴, C. Guyot¹³⁶, C. Gwenlan¹²⁰, C. B. Gwilliam⁷⁴, A. Haas¹¹⁰, C. Haber¹⁵, H. K. Hadavand⁸, N. Haddad^{135e}, P. Haefner²¹, S. Hageböck²¹, Z. Hajduk³⁹, H. Hakobyan¹⁷⁷, M. Haleem⁴², J. Haley¹¹⁴, D. Hall¹²⁰, G. Halladjian⁹⁰, G. D. Hallewell⁸⁵, K. Hamacher¹⁷⁵, P. Hamal¹¹⁵, K. Hamano¹⁶⁹, M. Hamer⁵⁴, A. Hamilton^{145a}, G. N. Hamity^{145c}, P. G. Hamnett⁴², L. Han^{33b}, K. Hanagaki¹¹⁸, K. Hanawa¹⁵⁵, M. Hance¹⁵, P. Hanke^{58a}, R. Hanna¹³⁶, J. B. Hansen³⁶, J. D. Hansen³⁶, M. C. Hansen²¹, P. H. Hansen³⁶, K. Hara¹⁶⁰, A. S. Hard¹⁷³, T. Harenberg¹⁷⁵, F. Hariri¹¹⁷, S. Harkusha⁹², R. D. Harrington⁴⁶, P. F. Harrison¹⁷⁰, F. Hartjes¹⁰⁷, M. Hasegawa⁶⁷, S. Hasegawa¹⁰³, Y. Hasegawa¹⁴⁰, A. Hasib¹¹³, S. Hassani¹³⁶, S. Haug¹⁷, R. Hauser⁹⁰, L. Hauswald⁴⁴, M. Havranek¹²⁷, C. M. Hawkes¹⁸, R. J. Hawkins³⁰, A. D. Hawkins⁸¹, T. Hayashi¹⁶⁰, D. Hayden⁹⁰, C. P. Hays¹²⁰, J. M. Hays⁷⁶, H. S. Hayward⁷⁴, S. J. Haywood¹³¹, S. J. Head¹⁸, T. Heck⁸³, V. Hedberg⁸¹, L. Heelan⁸, S. Heim¹²², T. Heim¹⁷⁵, B. Heinemann¹⁵, L. Heinrich¹¹⁰, J. Hejbal¹²⁷, L. Helary²², S. Hellman^{146a,146b}, D. Hellmich²¹, C. Helsens³⁰, J. Henderson¹²⁰, R. C. W. Henderson⁷², Y. Heng¹⁷³, C. Hengler⁴², A. Henrichs¹⁷⁶, A. M. Henriques Correia³⁰, S. Henrot-Versille¹¹⁷, G. H. Herbert¹⁶, Y. Hernández Jiménez¹⁶⁷, R. Herrberg-Schubert¹⁶, G. Herten⁴⁸, R. Hertenberger¹⁰⁰, L. Hervas³⁰, G. G. Hesketh⁷⁸, N. P. Hesse¹⁰⁷, J. W. Hetherly⁴⁰, R. Hickling⁷⁶, E. Higón-Rodríguez¹⁶⁷, E. Hill¹⁶⁹, J. C. Hill²⁸, K. H. Hiller⁴², S. J. Hillier¹⁸, I. Hinchliffe¹⁵, E. Hines¹²², R. R. Hinman¹⁵, M. Hirose¹⁵⁷, D. Hirschbuehl¹⁷⁵, J. Hobbs¹⁴⁸, N. Hod¹⁰⁷, M. C. Hodgkinson¹³⁹, P. Hodgson¹³⁹, A. Hoecker³⁰, M. R. Hoferkamp¹⁰⁵, F. Hoenig¹⁰⁰, M. Hohlfeld⁸³, D. Hohn²¹, T. R. Holmes¹⁵, M. Homann⁴³, T. M. Hong¹²⁵, L. Hooft van Huysduynen¹¹⁰, W. H. Hopkins¹¹⁶, Y. Horii¹⁰³, A. J. Horton¹⁴², J.-Y. Hostachy⁵⁵, S. Hou¹⁵¹, A. Hoummada^{135a}, J. Howard¹²⁰, J. Howarth⁴², M. Hrabovsky¹¹⁵, I. Hristova¹⁶, J. Hrivnac¹¹⁷, T. Hryn'ova⁵, A. Hrynevich⁹³, C. Hsu^{145c}, P. J. Hsu^{151,p}, S.-C. Hsu¹³⁸, D. Hu³⁵, Q. Hu^{33b}, X. Hu⁸⁹, Y. Huang⁴², Z. Hubacek³⁰, F. Hubaut⁸⁵, F. Huegging²¹, T. B. Huffman¹²⁰, E. W. Hughes³⁵, G. Hughes⁷², M. Huhtinen³⁰, T. A. Hülsing⁸³, N. Huseynov^{65,b}, J. Huston⁹⁰, J. Huth⁵⁷, G. Iacobucci⁴⁹, G. Iakovidis²⁵, I. Ibragimov¹⁴¹, L. Iconomidou-Fayard¹¹⁷, E. Ideal¹⁷⁶, Z. Idrissi^{135e}, P. Iengo³⁰, O. Igonkina¹⁰⁷, T. Iizawa¹⁷¹, Y. Ikegami⁶⁶, K. Ikematsu¹⁴¹, M. Ikeno⁶⁶, Y. Ilchenko^{31,q}, D. Iliadis¹⁵⁴, N. Ilic¹⁴³, Y. Inamaru⁶⁷, T. Ince¹⁰¹, P. Ioannou⁹, M. Iodice^{134a}, K. Iordanidou³⁵, V. Ippolito⁵⁷, A. Irlles Quiles¹⁶⁷, C. Isaksson¹⁶⁶, M. Ishino⁶⁸, M. Ishitsuka¹⁵⁷, R. Ishmukhametov¹¹¹, C. Issever¹²⁰, S. Istin^{19a}, J. M. Iturbe Ponce⁸⁴, R. Iuppa^{133a,133b}, J. Ivarsson⁸¹, W. Iwanski³⁹, H. Iwasaki⁶⁶, J. M. Izen⁴¹, V. Izzo^{104a}, S. Jabbar³, B. Jackson¹²², M. Jackson⁷⁴, P. Jackson¹, M. R. Jaekel³⁰, V. Jain², K. Jakobs⁴⁸, S. Jakobsen³⁰, T. Jakoubek¹²⁷,

J. Jakubek¹²⁸, D. O. Jamin¹⁵¹, D. K. Jana⁷⁹, E. Jansen⁷⁸, R. Jansky⁶², J. Janssen²¹, M. Janus¹⁷⁰, G. Jarlskog⁸¹, N. Javadov^{65,b}, T. Javůrek⁴⁸, L. Jeanty¹⁵, J. Jejelava^{51a,r}, G.-Y. Jeng¹⁵⁰, D. Jennens⁸⁸, P. Jenni^{48,s}, J. Jentsch⁴³, C. Jeske¹⁷⁰, S. Jézéquel⁵, H. Ji¹⁷³, J. Jia¹⁴⁸, Y. Jiang^{33b}, S. Jiggins⁷⁸, J. Jimenez Pena¹⁶⁷, S. Jin^{33a}, A. Jinaru^{26a}, O. Jinnouchi¹⁵⁷, M. D. Joergensen³⁶, P. Johansson¹³⁹, K. A. Johns⁷, K. Jon-And^{146a,146b}, G. Jones¹⁷⁰, R. W. L. Jones⁷², T. J. Jones⁷⁴, J. Jongmanns^{58a}, P. M. Jorge^{126a,126b}, K. D. Joshi⁸⁴, J. Jovicevic^{159a}, X. Ju¹⁷³, C. A. Jung⁴³, P. Jussel⁶², A. Juste Rozas^{12,o}, M. Kaci¹⁶⁷, A. Kaczmarek³⁹, M. Kado¹¹⁷, H. Kagan¹¹¹, M. Kagan¹⁴³, S. J. Kahn⁸⁵, E. Kajomovitz⁴⁵, C. W. Kalderon¹²⁰, S. Kama⁴⁰, A. Kamenshchikov¹³⁰, N. Kanaya¹⁵⁵, M. Kaneda³⁰, S. Kaneti²⁸, V. A. Kantserov⁹⁸, J. Kanzaki⁶⁶, B. Kaplan¹¹⁰, A. Kapliy³¹, D. Kar⁵³, K. Karakostas¹⁰, A. Karamaoun³, N. Karastathis^{10,107}, M. J. Kareem⁵⁴, M. Karneevskiy⁸³, S. N. Karpov⁶⁵, Z. M. Karpova⁶⁵, K. Karthik¹¹⁰, V. Kartvelishvili⁷², A. N. Karyukhin¹³⁰, L. Kashif¹⁷³, R. D. Kass¹¹¹, A. Kastanas¹⁴, Y. Kataoka¹⁵⁵, A. Katre⁴⁹, J. Katzy⁴², K. Kawagoe⁷⁰, T. Kawamoto¹⁵⁵, G. Kawamura⁵⁴, S. Kazama¹⁵⁵, V. F. Kazanin^{109,c}, M. Y. Kazarinov⁶⁵, R. Keeler¹⁶⁹, R. Kehoe⁴⁰, J. S. Keller⁴², J. J. Kempster⁷⁷, H. Keoshkerian⁸⁴, O. Kepka¹²⁷, B. P. Kerševan⁷⁵, S. Kersten¹⁷⁵, R. A. Keyes⁸⁷, F. Khalil-zada¹¹, H. Khandanyan^{146a,146b}, A. Khanov¹¹⁴, A. G. Kharlamov^{109,c}, T. J. Khoo²⁸, V. Khovanskii⁹⁷, E. Khramov⁶⁵, J. Khubua^{51b,t}, H. Y. Kim⁸, H. Kim^{146a,146b}, S. H. Kim¹⁶⁰, Y. K. Kim³¹, N. Kimura¹⁵⁴, O. M. Kind¹⁶, B. T. King⁷⁴, M. King¹⁶⁷, S. B. King¹⁶⁸, J. Kirk¹³¹, A. E. Kiryunin¹⁰¹, T. Kishimoto⁶⁷, D. Kisielewska^{38a}, F. Kiss⁴⁸, K. Kiuchi¹⁶⁰, O. Kivernyk¹³⁶, E. Kladiva^{144b}, M. H. Klein³⁵, M. Klein⁷⁴, U. Klein⁷⁴, K. Kleinknecht⁸³, P. Klimek^{146a,146b}, A. Klimentov²⁵, R. Klingenberg⁴³, J. A. Klinger¹³⁹, T. Klioutchnikova³⁰, E.-E. Kluge^{58a}, P. Kluit¹⁰⁷, S. Kluth¹⁰¹, E. Kneringer⁶², E. B. F. G. Knoops⁸⁵, A. Knue⁵³, A. Kobayashi¹⁵⁵, D. Kobayashi¹⁵⁷, T. Kobayashi¹⁵⁵, M. Kobel⁴⁴, M. Kocian¹⁴³, P. Kodys¹²⁹, T. Koffas²⁹, E. Koffeman¹⁰⁷, L. A. Kogan¹²⁰, S. Kohlmann¹⁷⁵, Z. Kohout¹²⁸, T. Kohriki⁶⁶, T. Koi¹⁴³, H. Kolanoski¹⁶, I. Koletsou⁵, A. A. Komar^{96,*}, Y. Komori¹⁵⁵, T. Kondo⁶⁶, N. Kondrashova⁴², K. Köneke⁴⁸, A. C. König¹⁰⁶, S. König⁸³, T. Kono^{66,u}, R. Konoplich^{110,v}, N. Konstantinidis⁷⁸, R. Kopeliansky¹⁵², S. Koperny^{38a}, L. Köpke⁸³, A. K. Kopp⁴⁸, K. Korcyl³⁹, K. Kordas¹⁵⁴, A. Korn⁷⁸, A. A. Korol^{109,c}, I. Korolkov¹², E. V. Korolkova¹³⁹, O. Kortner¹⁰¹, S. Kortner¹⁰¹, T. Kosek¹²⁹, V. V. Kostyukhin²¹, V. M. Kotov⁶⁵, A. Kotwal⁴⁵, A. Kourkoumeli-Charalampidi¹⁵⁴, C. Kourkoumelis⁹, V. Kouskoura²⁵, A. Koutsman^{159a}, R. Kowalewski¹⁶⁹, T. Z. Kowalski^{38a}, W. Kozanecki¹³⁶, A. S. Kozhin¹³⁰, V. A. Kramarenko⁹⁹, G. Kramberger⁷⁵, D. Krasnopevtsev⁹⁸, M. W. Krasny⁸⁰, A. Krasznahorkay³⁰, J. K. Kraus²¹, A. Kravchenko²⁵, S. Kreiss¹¹⁰, M. Kretz^{58c}, J. Kretzschmar⁷⁴, K. Kreutzfeldt⁵², P. Krieger¹⁵⁸, K. Krizka³¹, K. Kroeninger⁴³, H. Kroha¹⁰¹, J. Kroll¹²², J. Kroseberg²¹, J. Krstic¹³, U. Kruchonak⁶⁵, H. Krüger²¹, N. Krumnack⁶⁴, Z. V. Krumshcheyn⁶⁵, A. Kruse¹⁷³, M. C. Kruse⁴⁵, M. Kruskal²², T. Kubota⁸⁸, H. Kucuk⁷⁸, S. Kудay^{4b}, S. Kuehn⁴⁸, A. Kugel^{58c}, F. Kuger¹⁷⁴, A. Kuhl¹³⁷, T. Kuhl⁴², V. Kukhtin⁶⁵, Y. Kulchitsky⁹², S. Kuleshov^{32b}, M. Kuna^{132a,132b}, T. Kunigo⁶⁸, A. Kupco¹²⁷, H. Kurashige⁶⁷, Y. A. Kurochkin⁹², R. Kurumida⁶⁷, V. Kus¹²⁷, E. S. Kuwertz¹⁶⁹, M. Kuze¹⁵⁷, J. Kvita¹¹⁵, T. Kwan¹⁶⁹, D. Kyriazopoulos¹³⁹, A. La Rosa⁴⁹, J. L. La Rosa Navarro^{24d}, L. La Rotonda^{37a,37b}, C. Lacasta¹⁶⁷, F. Lacava^{132a,132b}, J. Lacey²⁹, H. Lacker¹⁶, D. Lacour⁸⁰, V. R. Lacuesta¹⁶⁷, E. Ladygin⁶⁵, R. Lafaye⁵, B. Laforge⁸⁰, T. Lagouri¹⁷⁶, S. Lai⁴⁸, L. Lambourne⁷⁸, S. Lammers⁶¹, C. L. Lampen⁷, W. Lampl⁷, E. Lançon¹³⁶, U. Landgraf⁴⁸, M. P. J. Landon⁷⁶, V. S. Lang^{58a}, J. C. Lange¹², A. J. Lankford¹⁶³, F. Lanni²⁵, K. Lantzsch³⁰, S. Laplace⁸⁰, C. Lapoire³⁰, J. F. Laporte¹³⁶, T. Lari^{91a}, F. Lasagni Manghi^{20a,20b}, M. Lassnig³⁰, P. Laurelli⁴⁷, W. Lavrijsen¹⁵, A. T. Law¹³⁷, P. Laycock⁷⁴, T. Lazovich⁵⁷, O. Le Dortz⁸⁰, E. Le Guirriec⁸⁵, E. Le Menedeu¹², M. LeBlanc¹⁶⁹, T. LeCompte⁶, F. Ledroit-Guillon⁵⁵, C. A. Lee^{145b}, S. C. Lee¹⁵¹, L. Lee¹, G. Lefebvre⁸⁰, M. Lefebvre¹⁶⁹, F. Legger¹⁰⁰, C. Leggett¹⁵, A. Lehan⁷⁴, G. Lehmann Miotto³⁰, X. Lei⁷, W. A. Leight²⁹, A. Leisos^{154,w}, A. G. Leister¹⁷⁶, M. A. L. Leite^{24d}, R. Leitner¹²⁹, D. Lellouch¹⁷², B. Lemmer⁵⁴, K. J. C. Leney⁷⁸, T. Lenz²¹, B. Lenzi³⁰, R. Leone⁷, S. Leone^{124a,124b}, C. Leonidopoulos⁴⁶, S. Leontsinis¹⁰, C. Leroy⁹⁵, C. G. Lester²⁸, M. Levchenko¹²³, J. Levêque⁵, D. Levin⁸⁹, L. J. Levinson¹⁷², M. Levy¹⁸, A. Lewis¹²⁰, A. M. Leyko²¹, M. Leyton⁴¹, B. Li^{33b,x}, H. Li¹⁴⁸, H. L. Li³¹, L. Li⁴⁵, L. Li^{33e}, S. Li⁴⁵, Y. Li^{33c,y}, Z. Liang¹³⁷, H. Liao³⁴, B. Liberti^{133a}, A. Liblong¹⁵⁸, P. Lichard³⁰, K. Lie¹⁶⁵, J. Liebal²¹, W. Liebig¹⁴, C. Limbach²¹, A. Limosani¹⁵⁰, S. C. Lin^{151,z}, T. H. Lin⁸³, F. Linde¹⁰⁷, B. E. Lindquist¹⁴⁸, J. T. Linnemann⁹⁰, E. Lipeles¹²², A. Lipniacka¹⁴, M. Lisovsky^{58b}, T. M. Liss¹⁶⁵, D. Lissauer²⁵, A. Lister¹⁶⁸, A. M. Litke¹³⁷, B. Liu^{151,aa}, D. Liu¹⁵¹, H. Liu⁸⁹, J. Liu⁸⁵, J. B. Liu^{33b}, K. Liu⁸⁵, L. Liu¹⁶⁵, M. Liu⁴⁵, M. Liu^{33b}, Y. Liu^{33b}, M. Livan^{121a,121b}, A. Lleres⁵⁵, J. Llorente Merino⁸², S. L. Lloyd⁷⁶, F. Lo Sterzo¹⁵¹, E. Lobodzinska⁴², P. Loch⁷, W. S. Lockman¹³⁷, F. K. Loebinger⁸⁴, A. E. Loevschall-Jensen³⁶, A. Loginov¹⁷⁶, T. Lohse¹⁶, K. Lohwasser⁴², M. Lokajicek¹²⁷, B. A. Long²², J. D. Long⁸⁹, R. E. Long⁷², K. A. Looper¹¹¹, L. Lopes^{126a}, D. Lopez Mateos⁵⁷, B. Lopez Paredes¹³⁹, I. Lopez Paz¹², J. Lorenz¹⁰⁰, N. Lorenzo Martinez⁶¹, M. Losada¹⁶², P. Loscutoff¹⁵, P. J. Lösel¹⁰⁰, X. Lou^{33a}, A. Lounis¹¹⁷, J. Love⁶, P. A. Love⁷², N. Lu⁸⁹, H. J. Lubatti¹³⁸, C. Luci^{132a,132b}, A. Lucotte⁵⁵, F. Luehring⁶¹, W. Lukas⁶², L. Luminari^{132a}, O. Lundberg^{146a,146b}, B. Lund-Jensen¹⁴⁷, D. Lynn²⁵, R. Lysak¹²⁷, E. Lytken⁸¹, H. Ma²⁵, L. L. Ma^{33d}, G. Maccarrone⁴⁷, A. Macchiolo¹⁰¹, C. M. Macdonald¹³⁹, J. Machado Miguens^{122,126b}, D. Macina³⁰, D. Madaffari⁸⁵, R. Madar³⁴, H. J. Maddocks⁷², W. F. Mader⁴⁴, A. Madsen¹⁶⁶, S. Maeland¹⁴, T. Maeno²⁵, A. Maevskiy⁹⁹, E. Magradze⁵⁴, K. Mahboubi⁴⁸,

J. Mahlstedt¹⁰⁷, C. Maiani¹³⁶, C. Maidantchik^{24a}, A. A. Maier¹⁰¹, T. Maier¹⁰⁰, A. Maio^{126a,126b,126d}, S. Majewski¹¹⁶, Y. Makida⁶⁶, N. Makovec¹¹⁷, B. Malaescu⁸⁰, Pa. Malecki³⁹, V. P. Maleev¹²³, F. Malek⁵⁵, U. Mallik⁶³, D. Malon⁶, C. Malone¹⁴³, S. Maltezos¹⁰, V. M. Malyshev¹⁰⁹, S. Malyukov³⁰, J. Mamuzic⁴², G. Mancini⁴⁷, B. Mandelli³⁰, L. Mandelli^{91a}, I. Mandić⁷⁵, R. Mandrysch⁶³, J. Maneira^{126a,126b}, A. Manfredini¹⁰¹, L. Manhaes de Andrade Filho^{24b}, J. Manjarres Ramos^{159b}, A. Mann¹⁰⁰, P. M. Manning¹³⁷, A. Manousakis-Katsikakis⁹, B. Mansoulie¹³⁶, R. Mantifel⁸⁷, M. Mantoani⁵⁴, L. Mapelli³⁰, L. March^{145c}, G. Marchiori⁸⁰, M. Marcisovsky¹²⁷, C. P. Marino¹⁶⁹, M. Marjanovic¹³, D. E. Marley⁸⁹, F. Marroquim^{24a}, S. P. Marsden⁸⁴, Z. Marshall¹⁵, L. F. Marti¹⁷, S. Marti-Garcia¹⁶⁷, B. Martin⁹⁰, T. A. Martin¹⁷⁰, V. J. Martin⁴⁶, B. Martin dit Latour¹⁴, M. Martinez^{12,o}, S. Martin-Haugh¹³¹, V. S. Martoiu^{26a}, A. C. Martyniuk⁷⁸, M. Marx¹³⁸, F. Marzano^{132a}, A. Marzin³⁰, L. Masetti⁸³, T. Mashimo¹⁵⁵, R. Mashinistov⁹⁶, J. Masik⁸⁴, A. L. Maslennikov^{109,c}, I. Massa^{20a,20b}, L. Massa^{20a,20b}, N. Massol⁵, P. Mastrandrea¹⁴⁸, A. Mastroberardino^{37a,37b}, T. Masubuchi¹⁵⁵, P. Mättig¹⁷⁵, J. Mattmann⁸³, J. Maurer^{26a}, S. J. Maxfield⁷⁴, D. A. Maximov^{109,c}, R. Mazini¹⁵¹, S. M. Mazza^{91a,91b}, L. Mazzaferro^{133a,133b}, G. Mc Goldrick¹⁵⁸, S. P. Mc Kee⁸⁹, A. McCarn⁸⁹, R. L. McCarthy¹⁴⁸, T. G. McCarthy²⁹, N. A. McCubbin¹³¹, K. W. McFarlane^{56,*}, J. A. McFayden⁷⁸, G. Mchedlidze⁵⁴, S. J. McMahon¹³¹, R. A. McPherson^{169,k}, M. Medinnis⁴², S. Meehan^{145a}, S. Mehlhase¹⁰⁰, A. Mehta⁷⁴, K. Meier^{58a}, C. Meineck¹⁰⁰, B. Meirose⁴¹, B. R. Mellado Garcia^{145c}, F. Meloni¹⁷, A. Mengarelli^{20a,20b}, S. Menke¹⁰¹, E. Meoni¹⁶¹, K. M. Mercurio⁵⁷, S. Mergelmeyer²¹, P. Mermod⁴⁹, L. Merola^{104a,104b}, C. Meroni^{91a}, F. S. Merritt³¹, A. Messina^{132a,132b}, J. Metcalfe²⁵, A. S. Mete¹⁶³, C. Meyer⁸³, C. Meyer¹²², J.-P. Meyer¹³⁶, J. Meyer¹⁰⁷, R. P. Middleton¹³¹, S. Miglioranza^{164a,164c}, L. Mijović²¹, G. Mikenberg¹⁷², M. Mikesikova¹²⁷, M. Mikuž⁷⁵, M. Milesi⁸⁸, A. Milic³⁰, D. W. Miller³¹, C. Mills⁴⁶, A. Milov¹⁷², D. A. Milstead^{146a,146b}, A. A. Minaenko¹³⁰, Y. Minami¹⁵⁵, I. A. Minashvili⁶⁵, A. I. Mincer¹¹⁰, B. Mindur^{38a}, M. Mineev⁶⁵, Y. Ming¹⁷³, L. M. Mir¹², T. Mitani¹⁷¹, J. Mitrevski¹⁰⁰, V. A. Mitsou¹⁶⁷, A. Miucci⁴⁹, P. S. Miyagawa¹³⁹, J. U. Mjörnmark⁸¹, T. Moa^{146a,146b}, K. Mochizuki⁸⁵, S. Mohapatra³⁵, W. Mohr⁴⁸, S. Molander^{146a,146b}, R. Moles-Valls¹⁶⁷, K. Mönig⁴², C. Monini⁵⁵, J. Monk³⁶, E. Monnier⁸⁵, J. Montejo Berlingen¹², F. Monticelli⁷¹, S. Monzani^{132a,132b}, R. W. Moore³, N. Morange¹¹⁷, D. Moreno¹⁶², M. Moreno Llacer⁵⁴, P. Morettini^{50a}, M. Morgenstern⁴⁴, M. Morii⁵⁷, M. Morinaga¹⁵⁵, V. Morisbak¹¹⁹, S. Moritz⁸³, A. K. Morley¹⁴⁷, G. Mornacchi³⁰, J. D. Morris⁷⁶, S. S. Mortensen³⁶, A. Morton⁵³, L. Morvaj¹⁰³, M. Mosidze^{51b}, J. Moss¹¹¹, K. Motohashi¹⁵⁷, R. Mount¹⁴³, E. Mountricha²⁵, S. V. Mouraviev^{96,*}, E. J. W. Moyse⁸⁶, S. Muanza⁸⁵, R. D. Mudd¹⁸, F. Mueller¹⁰¹, J. Mueller¹²⁵, K. Mueller²¹, R. S. P. Mueller¹⁰⁰, T. Mueller²⁸, D. Muenstermann⁴⁹, P. Mullen⁵³, G. A. Mullier¹⁷, Y. Munwes¹⁵³, J. A. Murillo Quijada¹⁸, W. J. Murray^{170,131}, H. Musheghyan⁵⁴, E. Musto¹⁵², A. G. Myagkov^{130,ab}, M. Myska¹²⁸, O. Nackenhorst⁵⁴, J. Nadal⁵⁴, K. Nagai¹²⁰, R. Nagai¹⁵⁷, Y. Nagai⁸⁵, K. Nagano⁶⁶, A. Nagarkar¹¹¹, Y. Nagasaka⁵⁹, K. Nagata¹⁶⁰, M. Nagel¹⁰¹, E. Nagy⁸⁵, A. M. Nairz³⁰, Y. Nakahama³⁰, K. Nakamura⁶⁶, T. Nakamura¹⁵⁵, I. Nakano¹¹², H. Namasivayam⁴¹, R. F. Naranjo Garcia⁴², R. Narayan³¹, T. Naumann⁴², G. Navarro¹⁶², R. Nayyar⁷, H. A. Neal⁸⁹, P. Yu. Nechaeva⁹⁶, T. J. Neep⁸⁴, P. D. Nef¹⁴³, A. Negri^{121a,121b}, M. Negrini^{20a}, S. Nektarijevic¹⁰⁶, C. Nellist¹¹⁷, A. Nelson¹⁶³, S. Nemecek¹²⁷, P. Nemethy¹¹⁰, A. A. Nepomuceno^{24a}, M. Nessi^{30,ac}, M. S. Neubauer¹⁶⁵, M. Neumann¹⁷⁵, R. M. Neves¹¹⁰, P. Nevski²⁵, P. R. Newman¹⁸, D. H. Nguyen⁶, R. B. Nickerson¹²⁰, R. Nicolaidou¹³⁶, B. Nicquevert³⁰, J. Nielsen¹³⁷, N. Nikiforou³⁵, A. Nikiforov¹⁶, V. Nikolaenko^{130,ab}, I. Nikolic-Audit⁸⁰, K. Nikolopoulos¹⁸, J. K. Nilsen¹¹⁹, P. Nilsson²⁵, Y. Ninomiya¹⁵⁵, A. Nisati^{132a}, R. Nisius¹⁰¹, T. Nobe¹⁵⁷, M. Nomachi¹¹⁸, I. Nomidis²⁹, T. Nooney⁷⁶, S. Norberg¹¹³, M. Nordberg³⁰, O. Novgorodova⁴⁴, S. Nowak¹⁰¹, M. Nozaki⁶⁶, L. Nozka¹¹⁵, K. Ntekas¹⁰, G. Nunes Hanninger⁸⁸, T. Nunnemann¹⁰⁰, E. Nurse⁷⁸, F. Nuti⁸⁸, B. J. O'Brien⁴⁶, F. O'Grady⁷, D. C. O'Neil¹⁴², V. O'Shea⁵³, F. G. Oakham^{29,d}, H. Oberlack¹⁰¹, T. Obermann²¹, J. Ocariz⁸⁰, A. Ochi⁶⁷, I. Ochoa⁷⁸, J. P. Ochoa-Ricoux^{32a}, S. Oda⁷⁰, S. Odaka⁶⁶, H. Ogren⁶¹, A. Oh⁸⁴, S. H. Oh⁴⁵, C. C. Ohm¹⁵, H. Ohman¹⁶⁶, H. Oide³⁰, W. Okamura¹¹⁸, H. Okawa¹⁶⁰, Y. Okumura³¹, T. Okuyama¹⁵⁵, A. Olariu^{26a}, S. A. Olivares Pino⁴⁶, D. Oliveira Damazio²⁵, E. Oliver Garcia¹⁶⁷, A. Olszewski³⁹, J. Olszowska³⁹, A. Onofre^{126a,126e}, P. U. E. Onyisi^{31,q}, C. J. Oram^{159a}, M. J. Oreglia³¹, Y. Oren¹⁵³, D. Orestano^{134a,134b}, N. Orlando¹⁵⁴, C. Oropeza Barrera⁵³, R. S. Orr¹⁵⁸, B. Osculati^{50a,50b}, R. Ospanov⁸⁴, G. Otero y Garzon²⁷, H. Otono⁷⁰, M. Ouchrif^{135d}, E. A. Ouellette¹⁶⁹, F. Ould-Saada¹¹⁹, A. Ouraou¹³⁶, K. P. Oussoren¹⁰⁷, Q. Ouyang^{33a}, A. Ovcharova¹⁵, M. Owen⁵³, R. E. Owen¹⁸, V. E. Ozcan^{19a}, N. Ozturk⁸, K. Pachal¹⁴², A. Pacheco Pages¹², C. Padilla Aranda¹², M. Pagáčová⁴⁸, S. Pagan Griso¹⁵, E. Paganis¹³⁹, C. Pahl¹⁰¹, F. Paige²⁵, P. Pais⁸⁶, K. Pajchel¹¹⁹, G. Palacino^{159b}, S. Palestini³⁰, M. Palka^{38b}, D. Pallin³⁴, A. Palma^{126a,126b}, Y. B. Pan¹⁷³, E. Panagiotopoulou¹⁰, C. E. Pandini⁸⁰, J. G. Panduro Vazquez⁷⁷, P. Pani^{146a,146b}, S. Panitkin²⁵, D. Pantea^{26a}, L. Paolozzi⁴⁹, Th. D. Papadopoulou¹⁰, K. Papageorgiou¹⁵⁴, A. Paramonov⁶, D. Paredes Hernandez¹⁵⁴, M. A. Parker²⁸, K. A. Parker¹³⁹, F. Parodi^{50a,50b}, J. A. Parsons³⁵, U. Parzefall⁴⁸, E. Pasqualucci^{132a}, S. Passaggio^{50a}, F. Pastore^{134a,134b,*}, Fr. Pastore⁷⁷, G. Pásztor²⁹, S. Patariaia¹⁷⁵, N. D. Patel¹⁵⁰, J. R. Pater⁸⁴, T. Pauly³⁰, J. Pearce¹⁶⁹, B. Pearson¹¹³, L. E. Pedersen³⁶, M. Pedersen¹¹⁹, S. Pedraza Lopez¹⁶⁷, R. Pedro^{126a,126b}, S. V. Peleganchuk^{109,c}, D. Pelikan¹⁶⁶, H. Peng^{33b}, B. Penning³¹, J. Penwell⁶¹, D. V. Perepelitsa²⁵, E. Perez Codina^{159a}, M. T. Pérez García-Estañ¹⁶⁷, L. Perini^{91a,91b}, H. Pernegger³⁰, S. Perrella^{104a,104b}, R. Peschke⁴², V. D. Peshekhonov⁶⁵, K. Peters³⁰, R. F. Y. Peters⁸⁴, B. A. Petersen³⁰, T. C. Petersen³⁶

E. Petit⁴², A. Petridis^{146a,146b}, C. Petridou¹⁵⁴, E. Petrolo^{132a}, F. Petrucci^{134a,134b}, N. E. Pettersson¹⁵⁷, R. Pezoa^{32b}, P. W. Phillips¹³¹, G. Piacquadio¹⁴³, E. Pianori¹⁷⁰, A. Picazio⁴⁹, E. Piccaro⁷⁶, M. Piccinini^{20a,20b}, M. A. Pickering¹²⁰, R. Piegai²⁷, D. T. Pignotti¹¹¹, J. E. Pilcher³¹, A. D. Pilkington⁸⁴, J. Pina^{126a,126b,126d}, M. Pinamonti^{164a,164c,ad}, J. L. Pinfold³, A. Pingel³⁶, B. Pinto^{126a}, S. Pires⁸⁰, M. Pitt¹⁷², C. Pizio^{91a,91b}, L. Plazak^{144a}, M.-A. Pleier²⁵, V. Pleskot¹²⁹, E. Plotnikova⁶⁵, P. Plucinski^{146a,146b}, D. Pluth⁶⁴, R. Poettgen^{146a,146b}, L. Poggioli¹¹⁷, D. Pohl²¹, G. Polesello^{121a}, A. Poley⁴², A. Policicchio^{37a,37b}, R. Polifka¹⁵⁸, A. Polini^{20a}, C. S. Pollard⁵³, V. Polychronakos²⁵, K. Pommès³⁰, L. Pontecorvo^{132a}, B. G. Pope⁹⁰, G. A. Popeneciu^{26b}, D. S. Popovic¹³, A. Poppleton³⁰, S. Pospisil¹²⁸, K. Potamianos¹⁵, I. N. Potrap⁶⁵, C. J. Potter¹⁴⁹, C. T. Potter¹¹⁶, G. Poulard³⁰, J. Poveda³⁰, V. Pozdnyakov⁶⁵, P. Pralavorio⁸⁵, A. Pranko¹⁵, S. Prasad³⁰, S. Prell⁶⁴, D. Price⁸⁴, L. E. Price⁶, M. Primavera^{73a}, S. Prince⁸⁷, M. Proissl⁴⁶, K. Prokofiev^{60c}, F. Prokoshin^{32b}, E. Protopapadaki¹³⁶, S. Protopopescu²⁵, J. Proudfoot⁶, M. Przybycien^{38a}, E. Ptacek¹¹⁶, D. Puddu^{134a,134b}, E. Pueschel⁸⁶, D. Puldon¹⁴⁸, M. Purohit^{25,ae}, P. Puzo¹¹⁷, J. Qian⁸⁹, G. Qin⁵³, Y. Qin⁸⁴, A. Quadt⁵⁴, D. R. Quarrie¹⁵, W. B. Quayle^{164a,164b}, M. Queitsch-Maitland⁸⁴, D. Quilty⁵³, S. Raddum¹¹⁹, V. Radeka²⁵, V. Radescu⁴², S. K. Radhakrishnan¹⁴⁸, P. Radloff¹¹⁶, P. Rados⁸⁸, F. Ragusa^{91a,91b}, G. Rahal¹⁷⁸, S. Rajagopalan²⁵, M. Rammensee³⁰, C. Rangel-Smith¹⁶⁶, F. Rauscher¹⁰⁰, S. Rave⁸³, T. Ravenscroft⁵³, M. Raymond³⁰, A. L. Read¹¹⁹, N. P. Readioff⁷⁴, D. M. Rebuffi^{121a,121b}, A. Redelbach¹⁷⁴, G. Redlinger²⁵, R. Reece¹³⁷, K. Reeves⁴¹, L. Rehnisch¹⁶, H. Reisin²⁷, M. Relich¹⁶³, C. Rembser³⁰, H. Ren^{33a}, A. Renaud¹¹⁷, M. Rescigno^{132a}, S. Resconi^{91a}, O. L. Rezanova^{109,c}, P. Reznicek¹²⁹, R. Rezvani⁹⁵, R. Richter¹⁰¹, S. Richter⁷⁸, E. Richter-Was^{38b}, O. Ricken²¹, M. Ridel⁸⁰, P. Rieck¹⁶, C. J. Riegel¹⁷⁵, J. Rieger⁵⁴, M. Rijssenbeek¹⁴⁸, A. Rimoldi^{121a,121b}, L. Rinaldi^{20a}, B. Ristić⁴⁹, E. Ritsch³⁰, I. Riu¹², F. Rizatdinova¹¹⁴, E. Rizvi⁷⁶, S. H. Robertson^{87,k}, A. Robichaud-Veronneau⁸⁷, D. Robinson²⁸, J. E. M. Robinson⁸⁴, A. Robson⁵³, C. Roda^{124a,124b}, S. Roe³⁰, O. Røhne¹¹⁹, S. Rolli¹⁶¹, A. Romaniouk⁹⁸, M. Romano^{20a,20b}, S. M. Romano Saez³⁴, E. Romero Adam¹⁶⁷, N. Rompotis¹³⁸, M. Ronzani⁴⁸, L. Roos⁸⁰, E. Ros¹⁶⁷, S. Rosati^{132a}, K. Rosbach⁴⁸, P. Rose¹³⁷, P. L. Rosendahl¹⁴, O. Rosenthal¹⁴¹, V. Rossetti^{146a,146b}, E. Rossi^{104a,104b}, L. P. Rossi^{50a}, R. Rosten¹³⁸, M. Rotaru^{26a}, I. Roth¹⁷², J. Rothberg¹³⁸, D. Rousseau¹¹⁷, C. R. Royon¹³⁶, A. Rozanov⁸⁵, Y. Rozen¹⁵², X. Ruan^{145c}, F. Rubbo¹⁴³, I. Rubinskiy⁴², V. I. Rud⁹⁹, C. Rudolph⁴⁴, M. S. Rudolph¹⁵⁸, F. Rühr⁴⁸, A. Ruiz-Martinez³⁰, Z. Rurikova⁴⁸, N. A. Rusakovich⁶⁵, A. Ruschke¹⁰⁰, H. L. Russell¹³⁸, J. P. Rutherford⁷, N. Ruthmann⁴⁸, Y. F. Ryabov¹²³, M. Rybar¹⁶⁵, G. Rybkin¹¹⁷, N. C. Ryder¹²⁰, A. F. Saavedra¹⁵⁰, G. Sabato¹⁰⁷, S. Sacerdoti²⁷, A. Saddique³, H. F.-W. Sadrozinski¹³⁷, R. Sadykov⁶⁵, F. Safai Tehrani^{132a}, M. Saimpert¹³⁶, H. Sakamoto¹⁵⁵, Y. Sakurai¹⁷¹, G. Salamanna^{134a,134b}, A. Salamon^{133a}, M. Saleem¹¹³, D. Salek¹⁰⁷, P. H. Sales De Bruin¹³⁸, D. Salihagic¹⁰¹, A. Salnikov¹⁴³, J. Salt¹⁶⁷, D. Salvatore^{37a,37b}, F. Salvatore¹⁴⁹, A. Salvucci¹⁰⁶, A. Salzburger³⁰, D. Sampsonidis¹⁵⁴, A. Sanchez^{104a,104b}, J. Sánchez¹⁶⁷, V. Sanchez Martinez¹⁶⁷, H. Sandaker¹¹⁹, R. L. Sandbach⁷⁶, H. G. Sander⁸³, M. P. Sanders¹⁰⁰, M. Sandhoff¹⁷⁵, C. Sandoval¹⁶², R. Sandstroem¹⁰¹, D. P. C. Sankey¹³¹, M. Sannino^{50a,50b}, A. Sansoni⁴⁷, C. Santoni³⁴, R. Santonico^{133a,133b}, H. Santos^{126a}, I. Santoyo Castillo¹⁴⁹, K. Sapp¹²⁵, A. Saprnov⁶⁵, J. G. Saraiva^{126a,126d}, B. Sarrazin²¹, O. Sasaki⁶⁶, Y. Sasaki¹⁵⁵, K. Sato¹⁶⁰, G. Sauvage^{5,*}, E. Sauvan⁵, G. Savage⁷⁷, P. Savard^{158,d}, C. Sawyer¹³¹, L. Sawyer^{79,n}, J. Saxon³¹, C. Sbarra^{20a}, A. Sbrizzi^{20a,20b}, T. Scanlon⁷⁸, D. A. Scannicchio¹⁶³, M. Scarcella¹⁵⁰, V. Scarfone^{37a,37b}, J. Schaarschmidt¹⁷², P. Schacht¹⁰¹, D. Schaefer³⁰, R. Schaefer⁴², J. Schaeffer⁸³, S. Schaepe²¹, S. Schaetzel^{58b}, U. Schäfer⁸³, A. C. Schaffer¹¹⁷, D. Schaile¹⁰⁰, R. D. Schamberger¹⁴⁸, V. Scharf^{58a}, V. A. Schegelsky¹²³, D. Scheirich¹²⁹, M. Schernau¹⁶³, C. Schiavi^{50a,50b}, C. Schillo⁴⁸, M. Schioppa^{37a,37b}, S. Schlenker³⁰, E. Schmidt⁴⁸, K. Schmieden³⁰, C. Schmitt⁸³, S. Schmitt^{58b}, S. Schmitt⁴², B. Schneider^{159a}, Y. J. Schnellbach⁷⁴, U. Schnoor⁴⁴, L. Schoeffel¹³⁶, A. Schoening^{58b}, B. D. Schoenrock⁹⁰, E. Schopf²¹, A. L. S. Schorlemmer⁵⁴, M. Schott⁸³, D. Schouten^{159a}, J. Schovancova⁸, S. Schramm⁴⁹, M. Schreyer¹⁷⁴, C. Schroeder⁸³, N. Schuh⁸³, M. J. Schultens²¹, H.-C. Schultz-Coulon^{58a}, H. Schulz¹⁶, M. Schumacher⁴⁸, B. A. Schumm¹³⁷, Ph. Schune¹³⁶, C. Schwanenberger⁸⁴, A. Schwartzman¹⁴³, T. A. Schwarz⁸⁹, Ph. Schwegler¹⁰¹, H. Schweiger⁸⁴, Ph. Schwemling¹³⁶, R. Schwienhorst⁹⁰, J. Schwindling¹³⁶, T. Schwindt²¹, F. G. Sciacca¹⁷, E. Scifo¹¹⁷, G. Sciolla²³, F. Scuri^{124a,124b}, F. Scutti²¹, J. Searcy⁸⁹, G. Sedov⁴², E. Sedykh¹²³, P. Seema²¹, S. C. Seidel¹⁰⁵, A. Seiden¹³⁷, F. Seifert¹²⁸, J. M. Seixas^{24a}, G. Sekhniaidze^{104a}, K. Sekhon⁸⁹, S. J. Sekula⁴⁰, D. M. Seliverstov^{123,*}, N. Semprini-Cesari^{20a,20b}, C. Serfon³⁰, L. Serin¹¹⁷, L. Serkin^{164a,164b}, T. Serre⁸⁵, M. Sessa^{134a,134b}, R. Seuster^{159a}, H. Severini¹¹³, T. Sfiligoi⁷⁵, F. Sforza³⁰, A. Sfyrla³⁰, E. Shabalina⁵⁴, M. Shamim¹¹⁶, L. Y. Shan^{33a}, R. Shang¹⁶⁵, J. T. Shank²², M. Shapiro¹⁵, P. B. Shatalov⁹⁷, K. Shaw^{164a,164b}, S. M. Shaw⁸⁴, A. Shcherbakova^{146a,146b}, C. Y. Shehu¹⁴⁹, P. Sherwood⁷⁸, L. Shi^{151,af}, S. Shimizu⁶⁷, C. O. Shimmin¹⁶³, M. Shimojima¹⁰², M. Shiyakova⁶⁵, A. Shmeleva⁹⁶, D. Shoaleh Saadi⁹⁵, M. J. Shochet³¹, S. Shojaii^{91a,91b}, S. Shrestha¹¹¹, E. Shulga⁹⁸, M. A. Shupe⁷, S. Shushkevich⁴², P. Sicho¹²⁷, O. Sidiropoulou¹⁷⁴, D. Sidorov¹¹⁴, A. Sidoti^{20a,20b}, F. Siegert⁴⁴, Dj. Sijacki¹³, J. Silva^{126a,126d}, Y. Silver¹⁵³, S. B. Silverstein^{146a}, V. Simak¹²⁸, O. Simard⁵, Lj. Simic¹³, S. Simion¹¹⁷, E. Simioni⁸³, B. Simmons⁷⁸, D. Simon³⁴, R. Simoniello^{91a,91b}, P. Sinervo¹⁵⁸, N. B. Sinev¹¹⁶, G. Siragusa¹⁷⁴, A. N. Sisakyan^{65,*}, S. Yu. Sivoklov⁹⁹, J. Sjölin^{146a,146b}, T. B. Sjursen¹⁴, M. B. Skinner⁷², H. P. Skottowe⁵⁷, P. Skubic¹¹³, M. Slater¹⁸, T. Slavicek¹²⁸, M. Slawinska¹⁰⁷, K. Sliwa¹⁶¹, V. Smakhtin¹⁷², B. H. Smart⁴⁶, L. Smestad¹⁴, S. Yu. Smirnov⁹⁸, Y. Smirnov⁹⁸

L. N. Smirnova^{99,ag}, O. Smirnova⁸¹, M. N. K. Smith³⁵, R. W. Smith³⁵, M. Smizanska⁷², K. Smolek¹²⁸, A. A. Snesarev⁹⁶, G. Snidero⁷⁶, S. Snyder²⁵, R. Sobie^{169,k}, F. Socher⁴⁴, A. Soffer¹⁵³, D. A. Soh^{151,af}, C. A. Solans³⁰, M. Solar¹²⁸, J. Solc¹²⁸, E. Yu. Soldatov⁹⁸, U. Soldevila¹⁶⁷, A. A. Solodkov¹³⁰, A. Soloshenko⁶⁵, O. V. Solovyanov¹³⁰, V. Solovyev¹²³, P. Sommer⁴⁸, H. Y. Song^{33b}, N. Soni¹, A. Sood¹⁵, A. Sopczak¹²⁸, B. Sopko¹²⁸, V. Sopko¹²⁸, V. Sorin¹², D. Sosa^{58b}, M. Sosebee⁸, C. L. Sotiropoulou^{124a,124b}, R. Soualah^{164a,164c}, A. M. Soukharev^{109,c}, D. South⁴², B. C. Sowden⁷⁷, S. Spagnolo^{73a,73b}, M. Spalla^{124a,124b}, F. Spanò⁷⁷, W. R. Spearman⁵⁷, F. Spettel¹⁰¹, R. Spighi^{20a}, G. Spigo³⁰, L. A. Spiller⁸⁸, M. Spousta¹²⁹, T. Spreitzer¹⁵⁸, R. D. St. Denis^{53,*}, S. Staerz⁴⁴, J. Stahlman¹²², R. Stamen^{58a}, S. Stamm¹⁶, E. Stanecka³⁹, C. Stanescu^{134a}, M. Stanescu-Bellu⁴², M. M. Stanitzki⁴², S. Stapnes¹¹⁹, E. A. Starchenko¹³⁰, J. Stark⁵⁵, P. Staroba¹²⁷, P. Starovoitov⁴², R. Staszewski³⁹, P. Stavina^{144a,*}, P. Steinberg²⁵, B. Stelzer¹⁴², H. J. Stelzer³⁰, O. Stelzer-Chilton^{159a}, H. Stenzel⁵², S. Stern¹⁰¹, G. A. Stewart⁵³, J. A. Stillings²¹, M. C. Stockton⁸⁷, M. Stoebe⁸⁷, G. Stoicea^{26a}, P. Stolte⁵⁴, S. Stonjek¹⁰¹, A. R. Stradling⁸, A. Straessner⁴⁴, M. E. Stramaglia¹⁷, J. Strandberg¹⁴⁷, S. Strandberg^{146a,146b}, A. Strandlie¹¹⁹, E. Strauss¹⁴³, M. Strauss¹¹³, P. Striznec^{144b}, R. Ströhmer¹⁷⁴, D. M. Strom¹¹⁶, R. Stroynowski⁴⁰, A. Strubig¹⁰⁶, S. A. Stucci¹⁷, B. Stugu¹⁴, N. A. Styles⁴², D. Su¹⁴³, J. Su¹²⁵, R. Subramaniam⁷⁹, A. Succurro¹², Y. Sugaya¹¹⁸, C. Suhr¹⁰⁸, M. Suk¹²⁸, V. V. Sulin⁹⁶, S. Sultansoy^{4c}, T. Sumida⁶⁸, S. Sun⁵⁷, X. Sun^{33a}, J. E. Sundermann⁴⁸, K. Suruliz¹⁴⁹, G. Susinno^{37a,37b}, M. R. Sutton¹⁴⁹, S. Suzuki⁶⁶, Y. Suzuki⁶⁶, M. Svatos¹²⁷, S. Swedish¹⁶⁸, M. Swiatlowski¹⁴³, I. Sykora^{144a}, T. Sykora¹²⁹, D. Ta⁹⁰, C. Taccini^{134a,134b}, K. Tackmann⁴², J. Taenzer¹⁵⁸, A. Taffard¹⁶³, R. Tafirout^{159a}, N. Taiblum¹⁵³, H. Takai²⁵, R. Takashima⁶⁹, H. Takeda⁶⁷, T. Takeshita¹⁴⁰, Y. Takubo⁶⁶, M. Talby⁸⁵, A. A. Talyshv^{109,c}, J. Y. C. Tam¹⁷⁴, K. G. Tan⁸⁸, J. Tanaka¹⁵⁵, R. Tanaka¹¹⁷, S. Tanaka⁶⁶, B. B. Tannenwald¹¹¹, N. Tannoury²¹, S. Tapprogge⁸³, S. Tarem¹⁵², F. Tarrade²⁹, G. F. Tartarelli^{91a}, P. Tas¹²⁹, M. Tasevsky¹²⁷, T. Tashiro⁶⁸, E. Tassi^{37a,37b}, A. Tavares Delgado^{126a,126b}, Y. Tayalati^{135d}, F. E. Taylor⁹⁴, G. N. Taylor⁸⁸, W. Taylor^{159b}, F. A. Teischinger³⁰, M. Teixeira Dias Castanheira⁷⁶, P. Teixeira-Dias⁷⁷, K. K. Temming⁴⁸, H. Ten Kate³⁰, P. K. Teng¹⁵¹, J. J. Teoh¹¹⁸, F. Tepel¹⁷⁵, S. Terada⁶⁶, K. Terashi¹⁵⁵, J. Terron⁸², S. Terzo¹⁰¹, M. Testa⁴⁷, R. J. Teuscher^{158,k}, J. Therhaag²¹, T. Theveneaux-Pelzer³⁴, J. P. Thomas¹⁸, J. Thomas-Wilsker⁷⁷, E. N. Thompson³⁵, P. D. Thompson¹⁸, R. J. Thompson⁸⁴, A. S. Thompson⁵³, L. A. Thomsen¹⁷⁶, E. Thomson¹²², M. Thomson²⁸, R. P. Thun^{89,*}, M. J. Tibbetts¹⁵, R. E. Ticse Torres⁸⁵, V. O. Tikhomirov^{96,ah}, Yu. A. Tikhonov^{109,c}, S. Timoshenko⁹⁸, E. Tiouchichine⁸⁵, P. Tipton¹⁷⁶, S. Tisserant⁸⁵, T. Todorov⁵, S. Todorova-Nova¹²⁹, J. Tojo⁷⁰, S. Tokár^{144a}, K. Tokushuku⁶⁶, K. Tollefson⁹⁰, E. Tolley⁵⁷, L. Tomlinson⁸⁴, M. Tomoto¹⁰³, L. Tompkins^{143,ai}, K. Toms¹⁰⁵, E. Torrence¹¹⁶, H. Torres¹⁴², E. Torró Pastor¹⁶⁷, J. Toth^{85,aj}, F. Touchard⁸⁵, D. R. Tovey¹³⁹, T. Trefzger¹⁷⁴, L. Tremblet³⁰, A. Tricoli³⁰, I. M. Trigger^{159a}, S. Trincaz-Duvoid⁸⁰, M. F. Tripiana¹², W. Trischuk¹⁵⁸, B. Trocme⁵⁵, C. Troncon^{91a}, M. Trottier-McDonald¹⁵, M. Trovatelli¹⁶⁹, P. True⁹⁰, L. Truong^{164a,164c}, M. Trzebinski³⁹, A. Trzupek³⁹, C. Tsarouchas³⁰, J. C-L. Tseng¹²⁰, P. V. Tsiareshka⁹², D. Tsiou¹⁵⁴, G. Tsiopolitis¹⁰, N. Tsirintanis⁹, S. Tsiskaridze¹², V. Tsiskaridze⁴⁸, E. G. Tskhadadze^{51a}, I. I. Tsukerman⁹⁷, V. Tsulaia¹⁵, S. Tsuno⁶⁶, D. Tsybychev¹⁴⁸, A. Tudorache^{26a}, V. Tudorache^{26a}, A. N. Tuna¹²², S. A. Tuppuri^{20a,20b}, S. Turchikhin^{99,ag}, D. Turecek¹²⁸, R. Turra^{91a,91b}, A. J. Turvey⁴⁰, P. M. Tuts³⁵, A. Tykhonov⁴⁹, M. Tylmad^{146a,146b}, M. Tyndel¹³¹, I. Ueda¹⁵⁵, R. Ueno²⁹, M. Ughetto^{146a,146b}, M. Ugland¹⁴, M. Uhlenbrock²¹, F. Ukegawa¹⁶⁰, G. Unal³⁰, A. Undrus²⁵, G. Unel¹⁶³, F. C. Ungaro⁴⁸, Y. Unno⁶⁶, C. Unverdorben¹⁰⁰, J. Urban^{144b}, P. Urquijo⁸⁸, P. Urrejola⁸³, G. Usai⁸, A. Usanova⁶², L. Vacavant⁸⁵, V. Vacek¹²⁸, B. Vachon⁸⁷, C. Valderanis⁸³, N. Valencic¹⁰⁷, S. Valentinetti^{20a,20b}, A. Valero¹⁶⁷, L. Valery¹², S. Valkar¹²⁹, E. Valladolid Gallego¹⁶⁷, S. Vallecorsa⁴⁹, J. A. Valls Ferrer¹⁶⁷, W. Van Den Wollenberg¹⁰⁷, P. C. Van Der Deijl¹⁰⁷, R. van der Geer¹⁰⁷, H. van der Graaf¹⁰⁷, R. Van Der Leeuw¹⁰⁷, N. van Eldik¹⁵², P. van Gemmeren⁶, J. Van Nieuwkoop¹⁴², I. van Vulpen¹⁰⁷, M. C. van Woerden³⁰, M. Vanadia^{132a,132b}, W. Vandelli³⁰, R. Vanguri¹²², A. Vaniachine⁶, F. Vannucci⁸⁰, G. Vardanyan¹⁷⁷, R. Vari^{132a}, E. W. Varnes⁷, T. Varol⁴⁰, D. Varouchas⁸⁰, A. Vartapetian⁸, K. E. Varvell¹⁵⁰, V. I. Vassilikopoulos⁵⁶, F. Vazeille³⁴, T. Vazquez Schroeder⁸⁷, J. Veatch⁷, L. M. Veloce¹⁵⁸, F. Veloso^{126a,126c}, T. Velz²¹, S. Veneziano^{132a}, A. Ventura^{73a,73b}, D. Ventura⁸⁶, M. Venturi¹⁶⁹, N. Venturi¹⁵⁸, A. Venturini²³, V. Vercesi^{121a}, M. Verducci^{132a,132b}, W. Verkerke¹⁰⁷, J. C. Vermeulen¹⁰⁷, A. Vest⁴⁴, M. C. Vetterli^{142,d}, O. Viazlo⁸¹, I. Vichou¹⁶⁵, T. Vickey¹³⁹, O. E. Vickey Boeriu¹³⁹, G. H. A. Viehhauser¹²⁰, S. Viel¹⁵, R. Vigne⁶², M. Villa^{20a,20b}, M. Villaplana Perez^{91a,91b}, E. Vilucchi⁴⁷, M. G. Vincker²⁹, V. B. Vinogradov⁶⁵, I. Vivarelli¹⁴⁹, F. Vives Vaque³, S. Vlachos¹⁰, D. Vladoiu¹⁰⁰, M. Vlasak¹²⁸, M. Vogel^{32a}, P. Vokac¹²⁸, G. Volpi^{124a,124b}, M. Volpi⁸⁸, H. von der Schmitt¹⁰¹, H. von Radziewski⁴⁸, E. von Toerne²¹, V. Vorobel¹²⁹, K. Vorobev⁹⁸, M. Vos¹⁶⁷, R. Voss³⁰, J. H. Vosseveld⁷⁴, N. Vranjes¹³, M. Vranjes Milosavljevic¹³, V. Vrba¹²⁷, M. Vreeswijk¹⁰⁷, R. Vuillemer³⁰, I. Vukotic³¹, Z. Vykydal¹²⁸, P. Wagner²¹, W. Wagner¹⁷⁵, H. Wahlberg⁷¹, S. Wahrmund⁴⁴, J. Wakabayashi¹⁰³, J. Walder⁷², R. Walker¹⁰⁰, W. Walkowiak¹⁴¹, C. Wang¹⁵¹, F. Wang¹⁷³, H. Wang¹⁵, H. Wang⁴⁰, J. Wang⁴², J. Wang^{33a}, K. Wang⁸⁷, R. Wang⁶, S. M. Wang¹⁵¹, T. Wang²¹, X. Wang¹⁷⁶, C. Wanotayaroj¹¹⁶, A. Warburton⁸⁷, C. P. Ward²⁸, D. R. Wardrope⁷⁸, M. Warsinsky⁴⁸, A. Washbrook⁴⁶, C. Wasicki⁴², P. M. Watkins¹⁸, A. T. Watson¹⁸, I. J. Watson¹⁵⁰, M. F. Watson¹⁸, G. Watts¹³⁸, S. Watts⁸⁴, B. M. Waugh⁷⁸, S. Webb⁸⁴, M. S. Weber¹⁷, S. W. Weber¹⁷⁴, J. S. Webster³¹, A. R. Weidberg¹²⁰, B. Weinert⁶¹, J. Weingarten⁵⁴, C. Weiser⁴⁸, H. Weits¹⁰⁷,

P. S. Wells³⁰, T. Wenaus²⁵, T. Wengler³⁰, S. Wenig³⁰, N. Wermes²¹, M. Werner⁴⁸, P. Werner³⁰, M. Wessels^{58a}, J. Wetter¹⁶¹, K. Whalen¹¹⁶, A. M. Wharton⁷², A. White⁸, M. J. White¹, R. White^{32b}, S. White^{124a,124b}, D. Whiteson¹⁶³, F. J. Wickens¹³¹, W. Wiedenmann¹⁷³, M. Wielers¹³¹, P. Wienemann²¹, C. Wiglesworth³⁶, L. A. M. Wiik-Fuchs²¹, A. Wildauer¹⁰¹, H. G. Wilkens³⁰, H. H. Williams¹²², S. Williams¹⁰⁷, C. Willis⁹⁰, S. Willocq⁸⁶, A. Wilson⁸⁹, J. A. Wilson¹⁸, I. Wingerter-Seez⁵, F. Winklmeier¹¹⁶, B. T. Winter²¹, M. Wittgen¹⁴³, J. Wittkowski¹⁰⁰, S. J. Wollstadt⁸³, M. W. Wolter³⁹, H. Wolters^{126a,126c}, B. K. Wosiek³⁹, J. Wotschack³⁰, M. J. Woudstra⁸⁴, K. W. Wozniak³⁹, M. Wu⁵⁵, M. Wu³¹, S. L. Wu¹⁷³, X. Wu⁴⁹, Y. Wu⁸⁹, T. R. Wyatt⁸⁴, B. M. Wynne⁴⁶, S. Xella³⁶, D. Xu^{33a}, L. Xu^{33b,ak}, B. Yabsley¹⁵⁰, S. Yacoob^{145b,al}, R. Yakabe⁶⁷, M. Yamada⁶⁶, Y. Yamaguchi¹¹⁸, A. Yamamoto⁶⁶, S. Yamamoto¹⁵⁵, T. Yamanaka¹⁵⁵, K. Yamauchi¹⁰³, Y. Yamazaki⁶⁷, Z. Yan²², H. Yang^{33e}, H. Yang¹⁷³, Y. Yang¹⁵¹, W.-M. Yao¹⁵, Y. Yasu⁶⁶, E. Yatsenko⁵, K. H. Yau Wong²¹, J. Ye⁴⁰, S. Ye²⁵, I. Yeletsikh⁶⁵, A. L. Yen⁵⁷, E. Yildirim⁴², K. Yorita¹⁷¹, R. Yoshida⁶, K. Yoshihara¹²², C. Young¹⁴³, C. J. S. Young³⁰, S. Youssef²², D. R. Yu¹⁵, J. Yu⁸, J. M. Yu⁸⁹, J. Yu¹¹⁴, L. Yuan⁶⁷, A. Yurkewicz¹⁰⁸, I. Yusuff^{28,am}, B. Zabinski³⁹, R. Zaidan⁶³, A. M. Zaitsev^{130,ab}, J. Zalieckas¹⁴, A. Zaman¹⁴⁸, S. Zambito⁵⁷, L. Zanello^{132a,132b}, D. Zanzi⁸⁸, C. Zeitnitz¹⁷⁵, M. Zeman¹²⁸, A. Zemla^{38a}, K. Zengel²³, O. Zenin¹³⁰, T. Ženiš^{144a}, D. Zerwas¹¹⁷, D. Zhang⁸⁹, F. Zhang¹⁷³, H. Zhang^{33c}, J. Zhang⁶, L. Zhang⁴⁸, R. Zhang^{33b}, X. Zhang^{33d}, Z. Zhang¹¹⁷, X. Zhao⁴⁰, Y. Zhao^{33d,117}, Z. Zhao^{33b}, A. Zhemchugov⁶⁵, J. Zhong¹²⁰, B. Zhou⁸⁹, C. Zhou⁴⁵, L. Zhou³⁵, L. Zhou⁴⁰, N. Zhou¹⁶³, C. G. Zhu^{33d}, H. Zhu^{33a}, J. Zhu⁸⁹, Y. Zhu^{33b}, X. Zhuang^{33a}, K. Zhukov⁹⁶, A. Zibell¹⁷⁴, D. Zieminska⁶¹, N. I. Zimine⁶⁵, C. Zimmermann⁸³, S. Zimmermann⁴⁸, Z. Zinonos⁵⁴, M. Zinser⁸³, M. Ziolkowski¹⁴¹, L. Živković¹³, G. Zobernig¹⁷³, A. Zoccoli^{20a,20b}, M. zur Nedden¹⁶, G. Zurzolo^{104a,104b}, L. Zwalinski³⁰

¹ Department of Physics, University of Adelaide, Adelaide, Australia

² Physics Department, SUNY Albany, Albany, NY, USA

³ Department of Physics, University of Alberta, Edmonton, AB, Canada

⁴ (a) Department of Physics, Ankara University, Ankara, Turkey; (b) Istanbul Aydin University, Istanbul, Turkey; (c) Division of Physics, TOBB University of Economics and Technology, Ankara, Turkey

⁵ LAPP, CNRS/IN2P3 and Université Savoie Mont Blanc, Annecy-le-Vieux, France

⁶ High Energy Physics Division, Argonne National Laboratory, Argonne, IL, USA

⁷ Department of Physics, University of Arizona, Tucson, AZ, USA

⁸ Department of Physics, The University of Texas at Arlington, Arlington, TX, USA

⁹ Physics Department, University of Athens, Athens, Greece

¹⁰ Physics Department, National Technical University of Athens, Zografou, Greece

¹¹ Institute of Physics, Azerbaijan Academy of Sciences, Baku, Azerbaijan

¹² Institut de Física d'Altes Energies and Departament de Física de la Universitat Autònoma de Barcelona, Barcelona, Spain

¹³ Institute of Physics, University of Belgrade, Belgrade, Serbia

¹⁴ Department for Physics and Technology, University of Bergen, Bergen, Norway

¹⁵ Physics Division, Lawrence Berkeley National Laboratory and University of California, Berkeley, CA, USA

¹⁶ Department of Physics, Humboldt University, Berlin, Germany

¹⁷ Albert Einstein Center for Fundamental Physics and Laboratory for High Energy Physics, University of Bern, Bern, Switzerland

¹⁸ School of Physics and Astronomy, University of Birmingham, Birmingham, UK

¹⁹ (a) Department of Physics, Bogazici University, Istanbul, Turkey; (b) Department of Physics Engineering, Gaziantep University, Gaziantep, Turkey; (c) Department of Physics, Dogus University, Gaziantep, Turkey

²⁰ (a) INFN Sezione di Bologna, Bologna, Italy; (b) Dipartimento di Fisica e Astronomia, Università di Bologna, Bologna, Italy

²¹ Physikalisches Institut, University of Bonn, Bonn, Germany

²² Department of Physics, Boston University, Boston, MA, USA

²³ Department of Physics, Brandeis University, Waltham, MA, USA

²⁴ (a) Universidade Federal do Rio De Janeiro COPPE/EE/IF, Rio de Janeiro, Brazil; (b) Electrical Circuits Department, Federal University of Juiz de Fora (UFJF), Juiz de Fora, Brazil; (c) Federal University of Sao Joao del Rei (UFSJ), Sao Joao del Rei, Brazil; (d) Instituto de Fisica, Universidade de Sao Paulo, São Paulo, Brazil

²⁵ Physics Department, Brookhaven National Laboratory, Upton, NY, USA

- 26 (a) National Institute of Physics and Nuclear Engineering, Bucharest, Romania; (b) Physics Department, National Institute for Research and Development of Isotopic and Molecular Technologies, Cluj Napoca, Romania; (c) University Politehnica Bucharest, Bucharest, Romania; (d) West University in Timisoara, Timisoara, Romania
- 27 Departamento de Física, Universidad de Buenos Aires, Buenos Aires, Argentina
- 28 Cavendish Laboratory, University of Cambridge, Cambridge, UK
- 29 Department of Physics, Carleton University, Ottawa, ON, Canada
- 30 CERN, Geneva, Switzerland
- 31 Enrico Fermi Institute, University of Chicago, Chicago, IL, USA
- 32 (a) Departamento de Física, Pontificia Universidad Católica de Chile, Santiago, Chile; (b) Departamento de Física, Universidad Técnica Federico Santa María, Valparaíso, Chile
- 33 (a) Institute of High Energy Physics, Chinese Academy of Sciences, Beijing, China; (b) Department of Modern Physics, University of Science and Technology of China, Hefei, Anhui, China; (c) Department of Physics, Nanjing University, Nanjing, Jiangsu, China; (d) School of Physics, Shandong University, Shandong, China; (e) Shanghai Key Laboratory for Particle Physics and Cosmology, Department of Physics and Astronomy, Shanghai Jiao Tong University, Shanghai, China; (f) Physics Department, Tsinghua University, Beijing 100084, China
- 34 Laboratoire de Physique Corpusculaire, Clermont Université and Université Blaise Pascal and CNRS/IN2P3, Clermont-Ferrand, France
- 35 Nevis Laboratory, Columbia University, Irvington, NY, USA
- 36 Niels Bohr Institute, University of Copenhagen, Copenhagen, Denmark
- 37 (a) INFN Gruppo Collegato di Cosenza, Laboratori Nazionali di Frascati, Frascati, Italy; (b) Dipartimento di Fisica, Università della Calabria, Rende, Italy
- 38 (a) AGH University of Science and Technology, Faculty of Physics and Applied Computer Science, Kraków, Poland; (b) Marian Smoluchowski Institute of Physics, Jagiellonian University, Kraków, Poland
- 39 Institute of Nuclear Physics, Polish Academy of Sciences, Kraków, Poland
- 40 Physics Department, Southern Methodist University, Dallas, TX, USA
- 41 Physics Department, University of Texas at Dallas, Richardson, TX, USA
- 42 DESY, Hamburg and Zeuthen, Germany
- 43 Institut für Experimentelle Physik IV, Technische Universität Dortmund, Dortmund, Germany
- 44 Institut für Kern- und Teilchenphysik, Technische Universität Dresden, Dresden, Germany
- 45 Department of Physics, Duke University, Durham, NC, USA
- 46 SUPA-School of Physics and Astronomy, University of Edinburgh, Edinburgh, UK
- 47 INFN Laboratori Nazionali di Frascati, Frascati, Italy
- 48 Fakultät für Mathematik und Physik, Albert-Ludwigs-Universität, Freiburg, Germany
- 49 Section de Physique, Université de Genève, Geneva, Switzerland
- 50 (a) INFN Sezione di Genova, Genoa, Italy; (b) Dipartimento di Fisica, Università di Genova, Genoa, Italy
- 51 (a) E. Andronikashvili Institute of Physics, Iv. Javakishvili Tbilisi State University, Tbilisi, Georgia; (b) High Energy Physics Institute, Tbilisi State University, Tbilisi, Georgia
- 52 II Physikalisches Institut, Justus-Liebig-Universität Giessen, Giessen, Germany
- 53 SUPA-School of Physics and Astronomy, University of Glasgow, Glasgow, UK
- 54 II Physikalisches Institut, Georg-August-Universität, Göttingen, Germany
- 55 Laboratoire de Physique Subatomique et de Cosmologie, Université Grenoble-Alpes, CNRS/IN2P3, Grenoble, France
- 56 Department of Physics, Hampton University, Hampton, VA, USA
- 57 Laboratory for Particle Physics and Cosmology, Harvard University, Cambridge, MA, USA
- 58 (a) Kirchhoff-Institut für Physik, Ruprecht-Karls-Universität Heidelberg, Heidelberg, Germany; (b) Physikalisches Institut, Ruprecht-Karls-Universität Heidelberg, Heidelberg, Germany; (c) ZITI Institut für technische Informatik, Ruprecht-Karls-Universität Heidelberg, Mannheim, Germany
- 59 Faculty of Applied Information Science, Hiroshima Institute of Technology, Hiroshima, Japan
- 60 (a) Department of Physics, The Chinese University of Hong Kong, Shatin, NT, Hong Kong; (b) Department of Physics, The University of Hong Kong, Hong Kong, Hong Kong; (c) Department of Physics, The Hong Kong University of Science and Technology, Clear Water Bay, Kowloon, Hong Kong, China
- 61 Department of Physics, Indiana University, Bloomington, IN, USA
- 62 Institut für Astro- und Teilchenphysik, Leopold-Franzens-Universität, Innsbruck, Austria
- 63 University of Iowa, Iowa City, IA, USA

- ⁶⁴ Department of Physics and Astronomy, Iowa State University, Ames, IA, USA
- ⁶⁵ Joint Institute for Nuclear Research, JINR Dubna, Dubna, Russia
- ⁶⁶ KEK, High Energy Accelerator Research Organization, Tsukuba, Japan
- ⁶⁷ Graduate School of Science, Kobe University, Kobe, Japan
- ⁶⁸ Faculty of Science, Kyoto University, Kyoto, Japan
- ⁶⁹ Kyoto University of Education, Kyoto, Japan
- ⁷⁰ Department of Physics, Kyushu University, Fukuoka, Japan
- ⁷¹ Instituto de Física La Plata, Universidad Nacional de La Plata and CONICET, La Plata, Argentina
- ⁷² Physics Department, Lancaster University, Lancaster, UK
- ⁷³ ^(a)INFN Sezione di Lecce, Lecce, Italy; ^(b)Dipartimento di Matematica e Fisica, Università del Salento, Lecce, Italy
- ⁷⁴ Oliver Lodge Laboratory, University of Liverpool, Liverpool, UK
- ⁷⁵ Department of Physics, Jožef Stefan Institute and University of Ljubljana, Ljubljana, Slovenia
- ⁷⁶ School of Physics and Astronomy, Queen Mary University of London, London, UK
- ⁷⁷ Department of Physics, Royal Holloway University of London, Surrey, UK
- ⁷⁸ Department of Physics and Astronomy, University College London, London, UK
- ⁷⁹ Louisiana Tech University, Ruston, LA, USA
- ⁸⁰ Laboratoire de Physique Nucléaire et de Hautes Energies, UPMC and Université Paris-Diderot and CNRS/IN2P3, Paris, France
- ⁸¹ Fysiska institutionen, Lunds universitet, Lund, Sweden
- ⁸² Departamento de Física Teórica C-15, Universidad Autónoma de Madrid, Madrid, Spain
- ⁸³ Institut für Physik, Universität Mainz, Mainz, Germany
- ⁸⁴ School of Physics and Astronomy, University of Manchester, Manchester, UK
- ⁸⁵ CPPM, Aix-Marseille Université and CNRS/IN2P3, Marseille, France
- ⁸⁶ Department of Physics, University of Massachusetts, Amherst, MA, USA
- ⁸⁷ Department of Physics, McGill University, Montreal, QC, Canada
- ⁸⁸ School of Physics, University of Melbourne, Melbourne, VIC, Australia
- ⁸⁹ Department of Physics, The University of Michigan, Ann Arbor, MI, USA
- ⁹⁰ Department of Physics and Astronomy, Michigan State University, East Lansing, MI, USA
- ⁹¹ ^(a)INFN Sezione di Milano, Milan, Italy; ^(b)Dipartimento di Fisica, Università di Milano, Milan, Italy
- ⁹² B.I. Stepanov Institute of Physics, National Academy of Sciences of Belarus, Minsk, Republic of Belarus
- ⁹³ National Scientific and Educational Centre for Particle and High Energy Physics, Minsk, Republic of Belarus
- ⁹⁴ Department of Physics, Massachusetts Institute of Technology, Cambridge, MA, USA
- ⁹⁵ Group of Particle Physics, University of Montreal, Montreal, QC, Canada
- ⁹⁶ P.N. Lebedev Institute of Physics, Academy of Sciences, Moscow, Russia
- ⁹⁷ Institute for Theoretical and Experimental Physics (ITEP), Moscow, Russia
- ⁹⁸ National Research Nuclear University MEPhI, Moscow, Russia
- ⁹⁹ D.V. Skobel'syn Institute of Nuclear Physics, M.V. Lomonosov Moscow State University, Moscow, Russia
- ¹⁰⁰ Fakultät für Physik, Ludwig-Maximilians-Universität München, Munich, Germany
- ¹⁰¹ Max-Planck-Institut für Physik (Werner-Heisenberg-Institut), Munich, Germany
- ¹⁰² Nagasaki Institute of Applied Science, Nagasaki, Japan
- ¹⁰³ Graduate School of Science and Kobayashi-Maskawa Institute, Nagoya University, Nagoya, Japan
- ¹⁰⁴ ^(a)INFN Sezione di Napoli, Naples, Italy; ^(b)Dipartimento di Fisica, Università di Napoli, Naples, Italy
- ¹⁰⁵ Department of Physics and Astronomy, University of New Mexico, Albuquerque, NM, USA
- ¹⁰⁶ Institute for Mathematics, Astrophysics and Particle Physics, Radboud University Nijmegen/Nikhef, Nijmegen, The Netherlands
- ¹⁰⁷ Nikhef National Institute for Subatomic Physics and University of Amsterdam, Amsterdam, The Netherlands
- ¹⁰⁸ Department of Physics, Northern Illinois University, De Kalb, IL, USA
- ¹⁰⁹ Budker Institute of Nuclear Physics, SB RAS, Novosibirsk, Russia
- ¹¹⁰ Department of Physics, New York University, New York, NY, USA
- ¹¹¹ Ohio State University, Columbus, OH, USA
- ¹¹² Faculty of Science, Okayama University, Okayama, Japan
- ¹¹³ Homer L. Dodge Department of Physics and Astronomy, University of Oklahoma, Norman, OK, USA
- ¹¹⁴ Department of Physics, Oklahoma State University, Stillwater, OK, USA

- ¹¹⁵ Palacký University, RCPTM, Olomouc, Czech Republic
- ¹¹⁶ Center for High Energy Physics, University of Oregon, Eugene, OR, USA
- ¹¹⁷ LAL, Université Paris-Sud and CNRS/IN2P3, Orsay, France
- ¹¹⁸ Graduate School of Science, Osaka University, Osaka, Japan
- ¹¹⁹ Department of Physics, University of Oslo, Oslo, Norway
- ¹²⁰ Department of Physics, Oxford University, Oxford, UK
- ¹²¹ ^(a)INFN Sezione di Pavia, Pavia, Italy; ^(b)Dipartimento di Fisica, Università di Pavia, Pavia, Italy
- ¹²² Department of Physics, University of Pennsylvania, Philadelphia, PA, USA
- ¹²³ National Research Centre “Kurchatov Institute” B.P.Konstantinov, Petersburg Nuclear Physics Institute, St. Petersburg, Russia
- ¹²⁴ ^(a)INFN Sezione di Pisa, Pisa, Italy; ^(b)Dipartimento di Fisica E. Fermi, Università di Pisa, Pisa, Italy
- ¹²⁵ Department of Physics and Astronomy, University of Pittsburgh, Pittsburgh, PA, USA
- ¹²⁶ ^(a)Laboratório de Instrumentação e Física Experimental de Partículas-LIP, Lisbon, Portugal; ^(b)Faculdade de Ciências, Universidade de Lisboa, Lisbon, Portugal; ^(c)Department of Physics, University of Coimbra, Coimbra, Portugal; ^(d)Centro de Física Nuclear da Universidade de Lisboa, Lisbon, Portugal; ^(e)Departamento de Física, Universidade do Minho, Braga, Portugal; ^(f)Departamento de Física Teórica y del Cosmos and CAFPE, Universidad de Granada, Granada, Spain; ^(g)Dep Física and CEFITEC of Faculdade de Ciências e Tecnologia, Universidade Nova de Lisboa, Caparica, Portugal
- ¹²⁷ Institute of Physics, Academy of Sciences of the Czech Republic, Prague, Czech Republic
- ¹²⁸ Czech Technical University in Prague, Prague, Czech Republic
- ¹²⁹ Faculty of Mathematics and Physics, Charles University in Prague, Prague, Czech Republic
- ¹³⁰ State Research Center Institute for High Energy Physics, Protvino, Russia
- ¹³¹ Particle Physics Department, Rutherford Appleton Laboratory, Didcot, UK
- ¹³² ^(a)INFN Sezione di Roma, Rome, Italy; ^(b)Dipartimento di Fisica, Sapienza Università di Roma, Rome, Italy
- ¹³³ ^(a)INFN Sezione di Roma Tor Vergata, Rome, Italy; ^(b)Dipartimento di Fisica, Università di Roma Tor Vergata, Rome, Italy
- ¹³⁴ ^(a)INFN Sezione di Roma Tre, Rome, Italy; ^(b)Dipartimento di Matematica e Fisica, Università Roma Tre, Rome, Italy
- ¹³⁵ ^(a)Faculté des Sciences Ain Chock, Réseau Universitaire de Physique des Hautes Energies-Université Hassan II, Casablanca, Morocco; ^(b)Centre National de l’Energie des Sciences Techniques Nucleaires, Rabat, Morocco; ^(c)Faculté des Sciences Semailia, Université Cadi Ayyad, LPHEA-Marrakech, Marrakech, Morocco; ^(d)Faculté des Sciences, Université Mohamed Premier and LTPM, Oujda, Morocco; ^(e)Faculté des Sciences, Université Mohammed V-Agdal, Rabat, Morocco
- ¹³⁶ DSM/IRFU (Institut de Recherches sur les Lois Fondamentales de l’Univers), CEA Saclay (Commissariat à l’Energie Atomique et aux Energies Alternatives), Gif-sur-Yvette, France
- ¹³⁷ Santa Cruz Institute for Particle Physics, University of California Santa Cruz, Santa Cruz, CA, USA
- ¹³⁸ Department of Physics, University of Washington, Seattle, WA, USA
- ¹³⁹ Department of Physics and Astronomy, University of Sheffield, Sheffield, UK
- ¹⁴⁰ Department of Physics, Shinshu University, Nagano, Japan
- ¹⁴¹ Fachbereich Physik, Universität Siegen, Siegen, Germany
- ¹⁴² Department of Physics, Simon Fraser University, Burnaby, BC, Canada
- ¹⁴³ SLAC National Accelerator Laboratory, Stanford, CA, USA
- ¹⁴⁴ ^(a)Faculty of Mathematics, Physics and Informatics, Comenius University, Bratislava, Slovak Republic; ^(b)Department of Subnuclear Physics, Institute of Experimental Physics of the Slovak Academy of Sciences, Kosice, Slovak Republic
- ¹⁴⁵ ^(a)Department of Physics, University of Cape Town, Cape Town, South Africa; ^(b)Department of Physics, University of Johannesburg, Johannesburg, South Africa; ^(c)School of Physics, University of the Witwatersrand, Johannesburg, South Africa
- ¹⁴⁶ ^(a)Department of Physics, Stockholm University, Stockholm, Sweden; ^(b)The Oskar Klein Centre, Stockholm, Sweden
- ¹⁴⁷ Physics Department, Royal Institute of Technology, Stockholm, Sweden
- ¹⁴⁸ Departments of Physics and Astronomy and Chemistry, Stony Brook University, Stony Brook, NY, USA
- ¹⁴⁹ Department of Physics and Astronomy, University of Sussex, Brighton, UK
- ¹⁵⁰ School of Physics, University of Sydney, Sydney, Australia
- ¹⁵¹ Institute of Physics, Academia Sinica, Taipei, Taiwan
- ¹⁵² Department of Physics, Technion: Israel Institute of Technology, Haifa, Israel

- 153 Raymond and Beverly Sackler School of Physics and Astronomy, Tel Aviv University, Tel Aviv, Israel
- 154 Department of Physics, Aristotle University of Thessaloniki, Thessaloniki, Greece
- 155 International Center for Elementary Particle Physics and Department of Physics, The University of Tokyo, Tokyo, Japan
- 156 Graduate School of Science and Technology, Tokyo Metropolitan University, Tokyo, Japan
- 157 Department of Physics, Tokyo Institute of Technology, Tokyo, Japan
- 158 Department of Physics, University of Toronto, Toronto, ON, Canada
- 159 ^(a)TRIUMF, Vancouver, BC, Canada; ^(b)Department of Physics and Astronomy, York University, Toronto, ON, Canada
- 160 Faculty of Pure and Applied Sciences, University of Tsukuba, Tsukuba, Japan
- 161 Department of Physics and Astronomy, Tufts University, Medford, MA, USA
- 162 Centro de Investigaciones, Universidad Antonio Narino, Bogotá, Colombia
- 163 Department of Physics and Astronomy, University of California Irvine, Irvine, CA, USA
- 164 ^(a)INFN Gruppo Collegato di Udine, Sezione di Trieste, Udine, Italy; ^(b)ICTP, Trieste, Italy; ^(c)Dipartimento di Chimica Fisica e Ambiente, Università di Udine, Udine, Italy
- 165 Department of Physics, University of Illinois, Urbana, IL, USA
- 166 Department of Physics and Astronomy, University of Uppsala, Uppsala, Sweden
- 167 Instituto de Física Corpuscular (IFIC) and Departamento de Física Atómica, Molecular y Nuclear and Departamento de Ingeniería Electrónica and Instituto de Microelectrónica de Barcelona (IMB-CNM), University of Valencia and CSIC, Valencia, Spain
- 168 Department of Physics, University of British Columbia, Vancouver, BC, Canada
- 169 Department of Physics and Astronomy, University of Victoria, Victoria, BC, Canada
- 170 Department of Physics, University of Warwick, Coventry, UK
- 171 Waseda University, Tokyo, Japan
- 172 Department of Particle Physics, The Weizmann Institute of Science, Rehovot, Israel
- 173 Department of Physics, University of Wisconsin, Madison, WI, USA
- 174 Fakultät für Physik und Astronomie, Julius-Maximilians-Universität, Würzburg, Germany
- 175 Fachbereich C Physik, Bergische Universität Wuppertal, Wuppertal, Germany
- 176 Department of Physics, Yale University, New Haven, CT, USA
- 177 Yerevan Physics Institute, Yerevan, Armenia
- 178 Centre de Calcul de l'Institut National de Physique Nucléaire et de Physique des Particules (IN2P3), Villeurbanne, France
- ^a Also at Department of Physics, King's College London, London, UK
- ^b Also at Institute of Physics, Azerbaijan Academy of Sciences, Baku, Azerbaijan
- ^c Also at Novosibirsk State University, Novosibirsk, Russia
- ^d Also at TRIUMF, Vancouver, BC, Canada
- ^e Also at Department of Physics, California State University, Fresno, CA, USA
- ^f Also at Department of Physics, University of Fribourg, Fribourg, Switzerland
- ^g Also at Departamento de Física e Astronomia, Faculdade de Ciências, Universidade do Porto, Porto, Portugal
- ^h Also at Tomsk State University, Tomsk, Russia
- ⁱ Also at CPPM, Aix-Marseille Université and CNRS/IN2P3, Marseille, France
- ^j Also at Università di Napoli Parthenope, Naples, Italy
- ^k Also at Institute of Particle Physics (IPP), Waterloo, Canada
- ^l Also at Particle Physics Department, Rutherford Appleton Laboratory, Didcot, UK
- ^m Also at Department of Physics, St. Petersburg State Polytechnical University, St. Petersburg, Russia
- ⁿ Also at Louisiana Tech University, Ruston, LA, USA
- ^o Also at Institutio Catalana de Recerca i Estudis Avancats, ICREA, Barcelona, Spain
- ^p Also at Department of Physics, National Tsing Hua University, Taiwan
- ^q Also at Department of Physics, The University of Texas at Austin, Austin, TX, USA
- ^r Also at Institute of Theoretical Physics, Ilia State University, Tbilisi, Georgia
- ^s Also at CERN, Geneva, Switzerland
- ^t Also at Georgian Technical University (GTU), Tbilisi, Georgia
- ^u Also at O Chadai Academic Production, Ochanomizu University, Tokyo, Japan
- ^v Also at Manhattan College, New York, NY, USA

- ^w Also at Hellenic Open University, Patras, Greece
- ^x Also at Institute of Physics, Academia Sinica, Taipei, Taiwan
- ^y Also at LAL, Université Paris-Sud and CNRS/IN2P3, Orsay, France
- ^z Also at Academia Sinica Grid Computing, Institute of Physics, Academia Sinica, Taipei, Taiwan
- ^{aa} Also at School of Physics, Shandong University, Shandong, China
- ^{ab} Also at Moscow Institute of Physics and Technology State University, Dolgoprudny, Russia
- ^{ac} Also at Section de Physique, Université de Genève, Geneva, Switzerland
- ^{ad} Also at International School for Advanced Studies (SISSA), Trieste, Italy
- ^{ae} Also at Department of Physics and Astronomy, University of South Carolina, Columbia, SC, USA
- ^{af} Also at School of Physics and Engineering, Sun Yat-sen University, Guangzhou, China
- ^{ag} Also at Faculty of Physics, M.V.Lomonosov Moscow State University, Moscow, Russia
- ^{ah} Also at National Research Nuclear University MEPhI, Moscow, Russia
- ^{ai} Also at Department of Physics, Stanford University, Stanford, CA, USA
- ^{aj} Also at Institute for Particle and Nuclear Physics, Wigner Research Centre for Physics, Budapest, Hungary
- ^{ak} Also at Department of Physics, The University of Michigan, Ann Arbor, MI, USA
- ^{al} Also at Discipline of Physics, University of KwaZulu-Natal, Durban, South Africa
- ^{am} Also at University of Malaya, Department of Physics, Kuala Lumpur, Malaysia

* Deceased